A RANDOM MATRIX MODEL FOR ELLIPTIC CURVE L-FUNCTIONS OF FINITE CONDUCTOR

E. DUEÑEZ, D.K. HUYNH, J.P. KEATING, S.J. MILLER, AND N.C. SNAITH

Abstract. We propose a random matrix model for families of elliptic curve L-functions of finite conductor. A repulsion of the critical zeros of these L-functions away from the center of the critical strip was observed numerically by S. J. Miller in 2006 [50]; such behaviour deviates qualitatively from the conjectural limiting distribution of the zeros (for large conductors this distribution is expected to approach the one-level density of eigenvalues of orthogonal matrices after appropriate rescaling). Our purpose here is to provide a random matrix model for Miller's surprising discovery. We consider the family of even quadratic twists of a given elliptic curve. The main ingredient in our model is a calculation of the eigenvalue distribution of random orthogonal matrices whose characteristic polynomials are larger than some given value at the symmetry point in the spectra. We call this sub-ensemble of $\mathrm{SO}(2N)$ the *excised orthogonal ensemble.* The sieving-off of matrices with small values of the characteristic polynomial is akin to the discretization of the central values of L-functions implied by the formulæ of Waldspurger and Kohnen-Zagier. The cut-off scale appropriate to modeling elliptic curve L-functions is exponentially small relative to the matrix size N. The one-level density of the excised ensemble can be expressed in terms of that of the well-known Jacobi ensemble, enabling the former to be explicitly calculated. It exhibits an exponentially small (on the scale of the mean spacing) hard gap determined by the cut-off value, followed by soft repulsion on a much larger scale. Neither of these features is present in the one-level density of $SO(2N)$. When $N \to \infty$ we recover the limiting orthogonal behaviour. Our results agree qualitatively with Miller's discrepancy. Choosing the cut-off appropriately gives a model in good quantitative agreement with the number-theoretical data.

Date: December 7, 2011.

2010 *Mathematics Subject Classification.* 11M26, 15B52 (primary), 11G05, 11G40, 15B10 (secondary).

Key words and phrases. Elliptic Curves, Low Lying Zeros, n-Level Statistics, Random Matrix Theory, Jacobi Ensembles, Characteristic Polynomial.

DKH was partially supported by EPSRC, a CRM postdoctoral fellowship and NSF grant DMS-0757627. SJM was partially supported by NSF grants DMS-0855257 and DMS-097006. NCS was partially supported by funding from EPSRC. The work of JPK and NCS was sponsored by the Air Force Office of Scientific Research, Air Force Material Command, USAF, under grant number FA8655-10-1-3088. The U.S. Government is authorized to reproduce and distribute reprints for Government purpose notwithstanding any copyright notation thereon. DKH, JPK and NCS are grateful to the Mathematical Sciences Research Institute (MSRI), Berkeley, for hospitality when this work and manuscript were completed.

1. Introduction

Understanding the ranks of elliptic curves is a central problem in number theory. The celebrated Birch and Swinnerton-Dyer conjecture provides an analytic approach to studying them via the order of vanishing of the associated L-functions at the centre of the critical strip: it states that the order of vanishing of the elliptic curve L-function at the central point equals the rank of the Mordell-Weil group. On the other hand, following the Katz-Sarnak philosophy, zero statistics of families of L-functions are conjectured to have an underlying symmetry type associated with certain random matrix ensembles [40, 41]: in an appropriate asymptotic limit, the statistics of the zeros of families of L-functions are modeled by (a subgroup of) one of the classical compact groups $\mathrm{U}(N)$, $\mathrm{O}(N)$ or $\mathrm{USp}(2N)$.

If we could model the order of vanishing for families of elliptic curve L-functions in terms of random matrices, then we would also gain information about the distribution of ranks within a family of elliptic curves via the Birch and Swinnerton-Dyer conjecture. This is the wider goal that motivates the current work.

There has been much success modelling families of L-functions with matrices from the classical compact groups [7, 8, 10–19, 21, 22, 25–35, 39–43, 47, 52–55, 57, 58], including families of elliptic curve L-functions [13, 14, 37, 38, 48, 49, 62]. This work strongly supports the Katz-Sarnak philosophy that, in the correct asymptotic limit, matrices from the classical compact groups accurately model the zero statistics of L-functions. Specifically, for families of elliptic curve L-functions it has been shown for restricted test-functions that the one- and two-level densities do indeed show the expected symmetry of orthogonal type[1], that is, of random matrices from $\mathrm{O}(N)$, in the limit of large conductor [48, 49, 62].

For the Riemann zeta function, and more generally families of L-functions, good qualitative agreement is also found, as the asymptotic limit is approached, by modeling the L-functions with finite-sized matrices where the matrix size is chosen so that the mean density of matrix eigenvalues matches the mean density of zeros of the L-functions under consideration (originally proposed by Keating and Snaith [42,43]). This finite matrix size model has been refined still further with the incorporation of number-theoretic information, leading to extremely convincing models for, for example, correlation functions [4, 6], spacing distributions [5], and moments and ratios of values of L-functions [11, 12].

However, in the elliptic curve case S. J. Miller, in numerical data gathered in [50], discovered a significant discrepancy from the scaling limit of the expected model of orthogonal matrices. That is, for elliptic curve L-functions of finite conductor there is a large (repulsive) deviation of the zero statistics from the expected orthogonal symmetry that is not explained by either using finite-size matrices or by the inclusion of arithmetical terms as in [4–6, 11, 12]. Miller was the first to discover the soft repulsion of zeros of elliptic curve L-functions from the central point, and his data is reproduced in figure 2. However, the larger data sets

[1] If the family has geometric rank r, then by the Birch and Swinnerton-Dyer conjecture and Silverman's specialization theorem all but finitely many of the elliptic curve L-functions have r zeros at the central point; the correct scaling limit is the limit of block diagonal orthogonal matrices with an $r \times r$ identity matrix as the upper left block.

of the present paper (see figure 4), along with the random matrix model, indicate a hard gap containing no zeros.[2] The specific goal of this paper is to present a model that accurately describes the zero statistics of elliptic curve L-functions of finite conductor.

The main ingredient in the new model is to mimic central values of elliptic curve L-functions by the value of the characteristic polynomial at 1 for matrices from $\mathrm{SO}(2N)$. The key fact about these central values, not previously incorporated into random matrix models for the zero statistics, is that they are either zero (for curves with rank greater than zero) or they are greater or equal to a finite minimal size fixed by arithmetical considerations. The characteristic polynomial of a matrix $A \in \mathrm{SO}(2N)$ is given by

$$\Lambda_A(e^{i\theta}, N) := \det(I - e^{i\theta}A^{-1}) = \prod_{k=1}^{N}(1 - e^{i(\theta-\theta_k)})(1 - e^{i(\theta+\theta_k)}), \tag{1.1}$$

with $e^{\pm i\theta_1}, \dots, e^{\pm i\theta_N}$ the eigenvalues of A. Motivated by the arithmetical size constraint on the central values of the L-functions we seek to understand, we here consider the set $T_{\mathcal{X}}$ of matrices $A \in \mathrm{SO}(2N)$ whose characteristic polynomial $\Lambda_A(1, N)$ is larger than some cut-off value $\exp(\mathcal{X})$. We call this the *excised orthogonal ensemble*. In figure 1 we plot the distribution of the first eigenvalue of $SO(24)$, which shows no repulsion, as well as the distribution of the first eigenvalue of an excised ensemble of 24×24 orthogonal matrices. Here the size of the excision is $\exp(\mathcal{X}) \approx 0.005$ and we see the hard gap at the origin where no eigenvalues lie, as well as the soft repulsion that interpolates between zero and the bulk of the distribution. This is seen more clearly in the right hand figure where a region near the origin is enlarged.

Recall that the one-level density $R_1^{G(N)}$ for a (circular) ensemble $G(N)$ of matrices whose eigenvalues are parametrized by an unordered N-tuple of eigenphases $\{\theta_n\}_1^N$ is given by

$$R_1^{G(N)}(\theta) = N \int \dots \int P(\theta, \theta_2, \dots, \theta_N) d\theta_2 \dots d\theta_N \tag{1.2}$$

where $P(\theta, \theta_2, \dots, \theta_N)$ is the joint probability density function of eigenphases[3]. Helpfully, the probability density function of the one-level density $R_1^{T_{\mathcal{X}}}$ can be expressed in terms of the well-known Jacobi ensemble J_N (see [24] for properties of this ensemble):

Theorem 1.1. *The one-level density $R_1^{T_{\mathcal{X}}}$ for the set $T_{\mathcal{X}}$ of matrices $A \in SO(2N)$ with characteristic polynomial $\Lambda_A(e^{i\theta}, N)$ satisfying $\log|\Lambda_A(1, N)| \geq \mathcal{X}$ is given by*

$$R_1^{T_{\mathcal{X}}}(\theta_1) = \frac{C_{\mathcal{X}}}{2\pi i}\int_{c-i\infty}^{c+i\infty} 2^{Nr}\frac{\exp(-r\mathcal{X})}{r} R_1^{J_N}(\theta_1; r - 1/2, -1/2) dr$$

[2]Subsequent to our posting this manuscript on the arXiv, Marshall [45] has developed a rigorous theory for this hard gap.

[3]Note that in the case of our interest, namely the (full, or excised) ensemble of orthogonal matrices of size $2N$, there are N pairs of eigenvalues parametrized by N eigenphases.

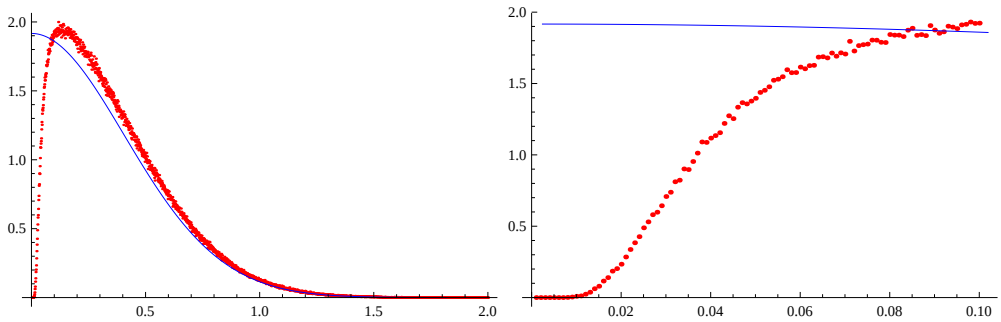

FIGURE 1. The distribution (blue, solid curve) of the first eigenvalue of $SO(24)$, showing no repulsion, and the distribution (red dots) of the first eigenvalue of an excised ensemble of 24×24 orthogonal matrices with $\exp(\mathcal{X}) \approx 0.005$. The right hand figure shows an enlargement near the origin. The $SO(24)$ curve is computed using the numerical differential equation solver for Painlevé VI which is developed in [20]. For the excised ensemble, 3 000 000 random $SO(24)$ matrices were generated and those not satisfying $\Lambda_A(1, N) \geq \exp(\mathcal{X})$ were discarded.

where $C_{\mathcal{X}}$ is a normalization constant defined in (6.12) and

$$R_1^{J_N}(\theta_1; r-1/2, -1/2) = N \int_0^\pi \cdots \int_0^\pi \prod_{j=1}^N w^{(r-1/2,-1/2)}(\cos\theta_j) \times \prod_{j<k} (\cos\theta_j - \cos\theta_k)^2 d\theta_2 \cdots d\theta_N \quad (1.3)$$

is the one-level density for the Jacobi ensemble J_N with weight function

$$w^{(\alpha,\beta)}(\cos\theta) = (1-\cos\theta)^{\alpha+1/2}(1+\cos\theta)^{\beta+1/2}, \qquad \alpha = r-1/2 \text{ and } \beta = -1/2.$$

Applying the method of orthogonal polynomials we evaluate $R_1^{J_N}(\theta; \alpha, \beta)$ to give

Theorem 1.2. *With $R_1^{T\mathcal{X}}$ as above, we have*

$$R_1^{T\mathcal{X}}(\theta) = \frac{C_{\mathcal{X}}}{2\pi i} \int_{c-i\infty}^{c+i\infty} \frac{\exp(-r\mathcal{X})}{r} 2^{N^2+2Nr-N} \times \times \prod_{j=0}^{N-1} \frac{\Gamma(2+j)\Gamma(1/2+j)\Gamma(r+1/2+j)}{\Gamma(r+N+j)} \times \times (1-\cos\theta)^r \frac{2^{1-r}}{2N+r-1} \frac{\Gamma(N+1)\Gamma(N+r)}{\Gamma(N+r-1/2)\Gamma(N-1/2)} P(N, r, \theta)\, dr \quad (1.4)$$

with normalization constant $C_{\mathcal{X}}$ defined in (6.12) and $P(N, r, \theta)$ defined in terms of Jacobi polynomials in (6.33).

An immediate consequence using residue calculus is the following:

Theorem 1.3. *With $R_1^{T_{\mathcal{X}}}$ as above, we have*

$$R_1^{T_{\mathcal{X}}}(\theta) = \begin{cases} 0 & \text{for } d(\theta,\mathcal{X}) < 0 \\ R_1^{\mathrm{SO}(2N)}(\theta) + C_{\mathcal{X}} \sum_{k=0}^{\infty} b_k(\theta) \exp((k+1/2)\mathcal{X}) & \text{for } d(\theta,\mathcal{X}) \geq 0, \end{cases} \tag{1.5}$$

where $d(\theta,\mathcal{X}) := (2N-1)\log 2 + \log(1-\cos\theta) - \mathcal{X}$ and b_k are coefficients arising from the residues. The normalization constant $C_{\mathcal{X}}$ is defined in (6.12) and $R_1^{\mathrm{SO}(2N)}(\theta)$ is the one-level density for $SO(2N)$, defined by (1.2).

Thus in the limit $\mathcal{X} \to -\infty$, θ fixed, $R_1^{T_{\mathcal{X}}}(\theta) \to R_1^{\mathrm{SO}(2N)}(\theta)$.

In order to compare our random matrix results with the elliptic curve data we shall need to take $-\mathcal{X}$ proportional to N, i.e. the cut-off is exponentially small in N. From Theorem 1.3, and illustrated in figure 13, one sees the existence of a hard gap where $R_1^{T_{\mathcal{X}}}(\theta)$ vanishes, namely the interval $\{\theta > 0 \mid d(\theta,\mathcal{X}) < 0\}$. When $-\mathcal{X} \propto N$ the hard gap is therefore exponentially small in N. Beyond this range the formula exhibits soft repulsion of the eigenvalues from 1 on a much larger scale; the repulsion extends far beyond the hard gap. It is interesting that such a 'pierced' subset of $\mathrm{SO}(2N)$, where the cut-off is exponentially small on the scale of the mean eigenvalue spacing, has such a pronounced effect on the eigenvalue statistics over a much larger distance.

This agrees qualitatively with the discrepancy Miller observed. We go on to discuss two ways to determine the relevant parameters which lead not just to qualitative but also quantitative agreement.

In the following sections we give some background information on elliptic curves (section 2.1), detail the anomalous zero statistics observed by Miller in [50] (section 2.2) and set out the new model (section 3). The model involves selecting from $\mathrm{SO}(2N)$ those matrices whose characteristic polynomial at 1 is larger than some given cut-off value (section 5.1). We apply the model with two matrix sizes: one the standard value related to the mean density of zeros and one an effective matrix size determined from lower-order terms of the one-level density (section 4). We present numerical evidence for our model using the distribution of the first zero of a family of elliptic curve L-functions (sections 5.2, 5.3) and also using the one-level density statistic for the excised ensemble of matrices (section 6).

2. Elliptic curve L-functions

2.1. **Background.** An elliptic curve E can be written in Weierstrass form as

$$y^2 + c_1xy + c_3y = x^3 + c_2x^2 + c_4x + c_6, \quad c_i \in \mathbb{Z}. \tag{2.1}$$

The L-function $L_E(s)$ associated with E is given by the Dirichlet series

$$L_E(s) = \sum_{n=1}^{\infty} \frac{\lambda(n)}{n^s}, \tag{2.2}$$

where the coefficients ($\lambda(n) = a(n)/\sqrt{n}$, with $a(p) = p + 1 - \#E(\mathbb{F}_p)$, $\#E(\mathbb{F}_p)$ being the number of points on E counted over $\mathbb{F}_p$), have been normalized so that

the functional equation relates s to $1-s$:

$$L_E(s) = \omega(E)\left(\frac{2\pi}{\sqrt{M}}\right)^{2s-1}\frac{\Gamma(3/2-s)}{\Gamma(s+1/2)}L_E(1-s). \tag{2.3}$$

Here M is the conductor of the elliptic curve E; for convenience we will consider only prime M. Also, $\omega(E)$ is $+1$ or -1 resulting, respectively, in an even or odd functional equation for L_E. There is a Generalized Riemann Hypothesis for L-functions of elliptic curves, stating that the non-trivial zeros of $L_E(s)$ lie on the critical line (with real part equal to $1/2$). The even (odd) symmetry of the functional equation implies an even (odd) symmetry of the zeros around the central point $s = 1/2$, where the critical line crosses the real axis. Often when we consider zeros statistics of a family of L-functions we are particularly interested in the zeros close to the central point.

The family of elliptic curve L-functions for which numerical evidence is presented in this paper is that of quadratic twists of a fixed curve E. Let $L_E(s,\chi_d)$ denote the L-function obtained by twisting $L_E(s)$ by a quadratic character χ_d. Here d is a fundamental discriminant, i.e., $d \in \mathbb{Z}$ such that $p^2 \nmid d$ for all odd primes p and $d \equiv 1 \bmod 4$ or $d \equiv 8, 12 \bmod 16$, and χ_d is the Kronecker symbol (an extension of the Legendre symbol, taking the values 1, 0, or -1). The twisted L-function, which is itself the L-function associated with another elliptic curve E_d, is given by

$$L_E(s,\chi_d) = \sum_{n=1}^{\infty}\frac{\lambda(n)\chi_d(n)}{n^s} = \prod_p\left(1 - \frac{\lambda(p)\chi_d(p)}{p^s} + \frac{\psi_M(p)\chi_d(p)^2}{p^{2s}}\right)^{-1}, \tag{2.4}$$

where ψ_M is the principal Dirichlet character of modulus M:

$$\psi_M(p) = \begin{cases} 1 \text{ if } p \nmid M \\ 0 \text{ otherwise.} \end{cases} \tag{2.5}$$

The functional equation of this L-function is, for $(d, M) = 1$,

$$L_E(s,\chi_d) = \chi_d(-M)\omega(E)\left(\frac{2\pi}{\sqrt{M}|d|}\right)^{2s-1}\frac{\Gamma(3/2-s)}{\Gamma(s+1/2)}L_E(1-s,\chi_d). \tag{2.6}$$

The sign of this functional equation is $\chi_d(-M)\omega(E)$ and it is more instructive to restrict to the fundamental discriminants which, for a fixed E, give an even, or alternatively an odd, functional equation for $L_E(s,\chi_d)$. In particular, the families we will consider in this paper will be denoted $\mathcal{F}_E^+(X)$: those quadratic twists of the curve E that have an even functional equation and $0 < d \le X$ (or else $-X \le d < 0$). In the appropriate asymptotic limit, zero statistics of families of L-functions of elliptic curves with even functional equation are believed to follow the distribution laws of eigenvalues of the even orthogonal group $\mathrm{SO}(2N)$ and those with odd functional equation are expected to show $\mathrm{SO}(2N+1)$ statistics.[4] The asymptotic parameter of the family $\mathcal{F}_E^+(X)$ is X. The conductor of $L_E(s,\chi_d)$ is Md^2, if M is the conductor of the original curve, and so d is the parameter that orders the curves by conductor. It is expected that as $X \to \infty$ the zero statistics of $\mathcal{F}_E^+(X)$ tend to the large-N limiting statistics of eigenvalues from

[4]If the family has rank then we must modify the random matrix ensemble as in Footnote 1.

$\mathrm{SO}(2N)$ in accordance with the Katz-Sarnak philosophy. We propose a model for the behaviour of zero statistics for finite X.

Key to this model are formulæ of Waldspurger [60], Kohnen-Zagier [44] and Baruch-Mao [3] which show that modular L-functions can only attain discrete values at the centre of the critical strip. In particular we have for the twists of an elliptic curve L-function

$$L_E(1/2, \chi_d) = \kappa_E \frac{c_E(|d|)^2}{d^{1/2}}, \tag{2.7}$$

where $c_E(|d|)$ are integers and the Fourier coefficients of a weight-3/2 modular form and κ_E is a constant depending on the curve E.

2.2. **Unexpected repulsion.** In 2006 S. J. Miller [50] investigated the statistics of the zeros of various families of elliptic curve L-functions. Figure 2 gives an example of what he discovered. It shows a histogram of the first zero above the central point for rank zero elliptic curve L-functions generated by randomly selecting the coefficients c_1 up to c_6 (as defined in (2.1)) for curves with conductors in the ranges indicated in the caption. The zeros are scaled by the mean density of low zeros of the L-functions and the plots are normalized so that they represent the probability density function for the first zero of L-functions from this family. Miller observes that there is clear repulsion of the first zero from the central point; that is, the plots drop to zero at the origin, indicating a very low probability of finding an L-function with a low first zero.

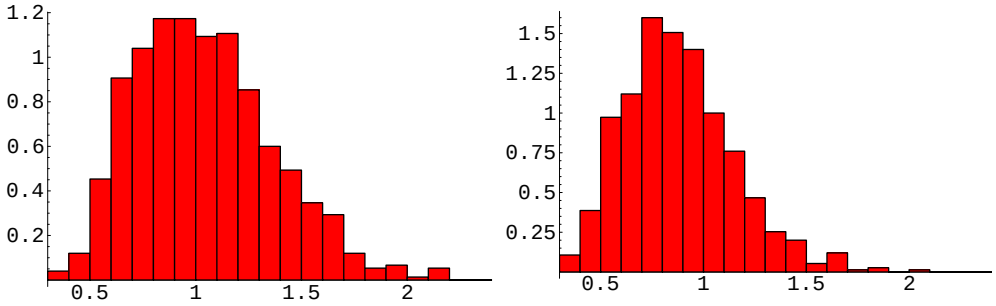

FIGURE 2. First normalized zero above the central point: Left: 750 rank 0 curves from $y^2+a_1xy+a_3y = x^3+a_2x^2+a_4x+a_6$, $\log(\mathrm{cond}) \in [3.2, 12.6]$, median = 1.00, mean = 1.04, standard deviation about the mean = .32. Right: 750 rank 0 curves from $y^2+a_1xy+a_3y = x^3+a_2x^2+a_4x+a_6$, $\log(\mathrm{cond}) \in [12.6, 14.9]$, median = .85, mean = .88, standard deviation about the mean = .27

What is surprising about these plots is that the standard way to model such L-functions would be with matrices from $\mathrm{SO}(2N)$, with N chosen to be equal to half the logarithm of the conductor of the curve. This choice of N has the effect of equating the density of eigenvalues to the density of zeros near the critical point and there has been much work showing, for the Riemann zeta function [15, 17–19, 22, 27, 29, 31, 33, 42, 47] and for families of L-functions not necessarily associated with elliptic curves [7, 8, 10–14, 16, 17, 34, 43, 58], that this can be

effective at modelling number-theoretic data even far from the asymptotic limit specified by Katz and Sarnak. However, as figure 3 illustrates, even for small-size $\mathrm{SO}(2N)$ matrices, the distribution of the eigenvalue closest to 1 on the unit circle (the random matrix equivalent to the distribution of the first zero of L-functions) shows no repulsion at the origin of the distribution —a fact of course well-known in random matrix theory.

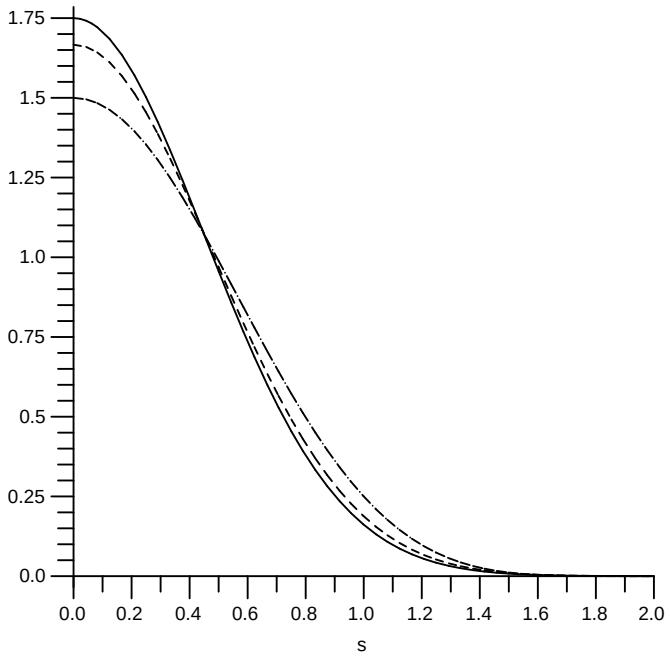

FIGURE 3. Probability density of normalized eigenvalue closest to 1 for SO(8) (solid), SO(6) (dashed) and SO(4) (dot-dashed).

This, then, is the mystery. No one doubts that in the large-conductor limit the distribution of the first zero of elliptic curve L-functions will tend to the large-N limit of the distribution of the first eigenvalues of $\mathrm{SO}(2N)$ matrices: Miller observes (see figure 2) that the repulsion decreases with increasing conductor. However, for finite conductor we do not get qualitative agreement with the statistics of finite-sized matrices, as we do in many other families of L-functions. Indeed one sees a qualitatively unexpected phenomenon, namely, repulsion of zeros away from the central point. In section 3 we outline an idea that successfully models the anomalous statistical behaviour discovered by Miller.

In this paper we concentrate on developing a model for the unexpected zero statistics of rank zero curves seen in figure 2. However, it should be noted that Miller [50] also investigated zeros of higher rank curves and the behaviour of zeros further from the central point, which will guide future attempts to model statistics of L-functions associated to elliptic curves of higher rank. Briefly, the numerical findings were the following:

(1) The repulsion of the low-lying zeros increased with increasing rank, and was present even for rank 0 curves.
(2) As the conductors increased, the repulsion decreased.
(3) Statistical tests failed to reject the hypothesis that, on average, the first three zeros were all repelled equally (i. e., shifted by the same amount).

3. The model

We propose to model the zero statistics of rank-zero elliptic curve L-functions with the subset $T_{\mathcal{X}}$ of $SO(2N)$ defined in the introduction. The justification for employing an *excised* random matrix model such as this is that formula (2.7) indicates that the L-functions themselves have a discretization at the central point. Thus the statement

$$L_E(1/2, \chi_d) < \frac{\kappa_E}{d^{1/2}} \tag{3.1}$$

implies that

$$L_E(1/2, \chi_d) = 0. \tag{3.2}$$

Hence, each $L_E(s, \chi_d) \in \mathcal{F}_E^+$ associated with a rank 0 curve E_d satisfies

$$L_E(1/2, \chi_d) \geq \frac{\kappa_E}{d^{1/2}}. \tag{3.3}$$

Thus, since previous work [10, 13, 14, 43] shows that values of L-functions at the central point can be characterized using characteristic polynomials evaluated at the point 1, to model rank 0 curves we discard from our orthogonal ensemble all matrices not satisfying (3.4) and we will propose a value of $\mathcal{X}$ based on (3.3). For a start, if we are working with discriminants of size around d then equating the density of eigenvalues, N/π, with that of zeros near the central point, $\frac{1}{\pi}\log(\frac{\sqrt{M}d}{2\pi})$, gives us an equivalent value of N: $N_{\text{std}} \sim \log d$. Since the L-values are discretized on a scale of $1/\sqrt{d}$, we "excise" (i. e., discard), characteristic polynomials whose value at 1 is of the scale $\exp(-N_{\text{std}}/2)$.

Thus, for certain values of N we plan to model elliptic curve zero statistics using matrices from $\mathrm{SO}(2N)$ satisfying

$$|\Lambda_A(1, N)| \geq \exp \mathcal{X} = c \times \exp(-N_{\text{std}}/2), \tag{3.4}$$

and we will propose a value for c in section 5.1. We present the model for the zero statistics using two different matrix sizes. One obvious choice is $N = N_{\text{std}}$ and we present data for this case in section 5.2. The other choice is an "effective" matrix size, N_{eff}, that incorporates arithmetic information and is based on an idea of Bogomolny, Bohigas, Leboeuf and Monastra [5]. We illustrate how N_{eff} is calculated in section 4 and present the numerical results of the model in section 5.3. In this paper we compare this model with numerical data from a family of twists of one particular elliptic curve, E_{11}.

4. lower-order terms and the effective matrix size

By the Katz-Sarnak philosophy the statistical properties of zeros of L-functions should asymptotically behave like the scaling limits of eigenvalues of random matrices drawn from one of the classical compact groups. However, for finite values of

the asymptotic parameter we observe deviations (of number-theoretic origin) from the limiting result. We note that for many families of L-functions these deviations, at least over length scales on the order of the mean spacing of zeros, are slight perturbations of the limiting results, in contrast to the elliptic curve case where we see distinct, qualitative disagreement (the repulsion at the central point).[5]

In this section we adapt the method of Bogomolny, Bohigas, Leboeuf and Monastra [5], previously used to investigate statistics of zeros of the Riemann zeta function at a finite height on the critical line, and apply it to the family $\mathcal{F}_E^+(X)$ of elliptic curve L-functions.

Specifically, Bogomolny *et al.* use a conjectured formula for the two-point correlation function of the Riemann zeros at finite height on the critical line [6] and compare it to the finite-N form of the two point correlation function of unitary matrices from $\mathrm{U}(N)$. Under the standard procedure of equating mean densities of eigenvalues with the mean density of zeros, yielding in this case

$$N = \log\left(\frac{T}{2\pi}\right), \tag{4.1}$$

the leading order term of these two formulæ match up, but Bogomolny *et al.* show that by looking at a scaled version of the statistic and then choosing an "effective" matrix size, related to N by multiplication by a constant of arithmetic origin, they can match the first lower-order term in the formulæ. By scaling a further variable they match yet another lower-order term, although this step requires that the considered Riemann zeros be high lying, a point we will return to later. The authors illustrate with comprehensive numerical results that with each successive refinement the fit of the random-matrix model to the Riemann zero data significantly improves. What is remarkable about this is that they don't just see good numerical agreement in the two-point correlation statistic, where good agreement is to be expected as terms were matched by design, but also in the nearest-neighbour spacing distribution. The nearest neighbour spacing statistic is the probability density for distances between consecutive zeros, or equivalently, a normalized histogram of gaps between consecutive zeros. The argument is that the corrections to the asymptotics in the form of N_{eff} and the further scaling factor is also valid for all correlation functions, and therefore also for the nearest neighbour spacing. The strength of this work is that using this heuristic approach the information gained from a simpler statistic (two-point correlation) yields information for a more complicated one (nearest-neighbour spacing)—the latter one being determined by all correlation functions together.

In the following we adopt the above method and apply it to the case of $\mathcal{F}_E^+(X)$. In this case we have a conjectural formula for the one-level density for the scaled zeros of $\mathcal{F}_E^+(X)$, as derived in [37, 38]. For our purposes this is best given as the

[5]Random matrix theory does not see the fine arithmetic properties of the family, which surface in the lower-order terms. Thus, while the main terms of various families of elliptic curves are the same, the lower-order terms show differences due, for instance, to complex multiplication or torsion points; see [51].

following expansion for large X (equation (3.18) in [37]):

$$\begin{aligned}&\frac{1}{X^*}\sum_{\substack{0<d\le X\\ \chi_d(-M)\omega_E=+1}}\sum_{\gamma_d} g\Big(\frac{\gamma_d L}{\pi}\Big)\\ &=\int_{-\infty}^{\infty} g(\tau)\left(1+\frac{\sin(2\pi\tau)}{2\pi\tau}-r_1\frac{1+\cos(2\pi\tau)}{L}-r_2\frac{\pi\tau\sin(2\pi\tau)}{L^2}\right)d\tau+O\left(\frac{1}{L^3}\right)\end{aligned} \tag{4.2}$$

with

$$L=\log\left(\frac{\sqrt{M}X}{2\pi}\right), \tag{4.3}$$

where γ_d is the imaginary part of a generic zero of $L_E(s,\chi_d)$, the sum is over fundamental discriminants d, and X^* is the number of fundamental discriminants satisfying the conditions on the sum. The coefficients r_1 and r_2 in (4.2) are arithmetic constants involving the Dirichlet coefficients of $L_E(s)$; see [37] for details.

As expected the result (4.2) has the form of the asymptotic random-matrix result

$$\widetilde{R}_1(s)=1+\left(\frac{\sin 2\pi s}{2\pi s}\right) \tag{4.4}$$

for the even orthogonal group, plus correction terms. We compare this expansion with the one we obtain by expanding the scaled one-level density of SO($2N$) for finite N. The unscaled one-level density of SO($2N$) is (see, for example, [9])

$$R_1(s)=\frac{2N-1}{2\pi}+\frac{\sin((2N-1)s)}{2\pi\sin s}, \tag{4.5}$$

and so scaling by the mean density and expanding in powers of $1/N$ gives

$$\frac{\pi}{N}R_1\left(\frac{\pi y}{N}\right)=1+\frac{\sin(2\pi y)}{2\pi y}-\frac{1+\cos(2\pi y)}{2N}-\frac{\pi y\sin(2\pi y)}{6N^2}+O\left(\frac{1}{N^3}\right). \tag{4.6}$$

By choosing an effective matrix size

$$N_{\text{eff}}=\frac{L}{2r_1} \tag{4.7}$$

we match the next-to-leading term in (4.2) and (4.6). Arguing as Bogomolny *et al.* we conjecture that the improvement made by using matrices of size N_{eff} also holds for all n-point correlation or density functions. In particular we apply this result to the distribution of the lowest zero and see significantly better agreement in the bulk and tail of the distribution when we use N_{eff} as opposed to the use of the standard matrix size $N_{\text{std}}=L$.

We illustrate the effect of N_{eff} in figure 4. We choose the elliptic curve E_{11} ($(c_1,c_2,c_3,c_4,c_6)=(0,-1,1,0,0)$ in Weierstrass form) and find numerically that, for this curve,

$$r_1\approx 2.8600. \tag{4.8}$$

We used Rubinstein's lcalc [56] to compute the lowest zero of the quadratic twists $L_{E_{11}}(s, \chi_d)$ with even functional equation and with fundamental discriminants d, $0 < d \leq X = 400{,}000$. The standard matrix size corresponding to $X = 400{,}000$ is

$$N_{\text{std}} = \log\left(\frac{\sqrt{11}X}{2\pi}\right) \approx 12.26, \tag{4.9}$$

whereas the effective one is

$$N_{\text{eff}} = \frac{N_{\text{std}}}{2r_1} \approx 2.14. \tag{4.10}$$

The distribution of the lowest zero (a normalized histogram of the heights of

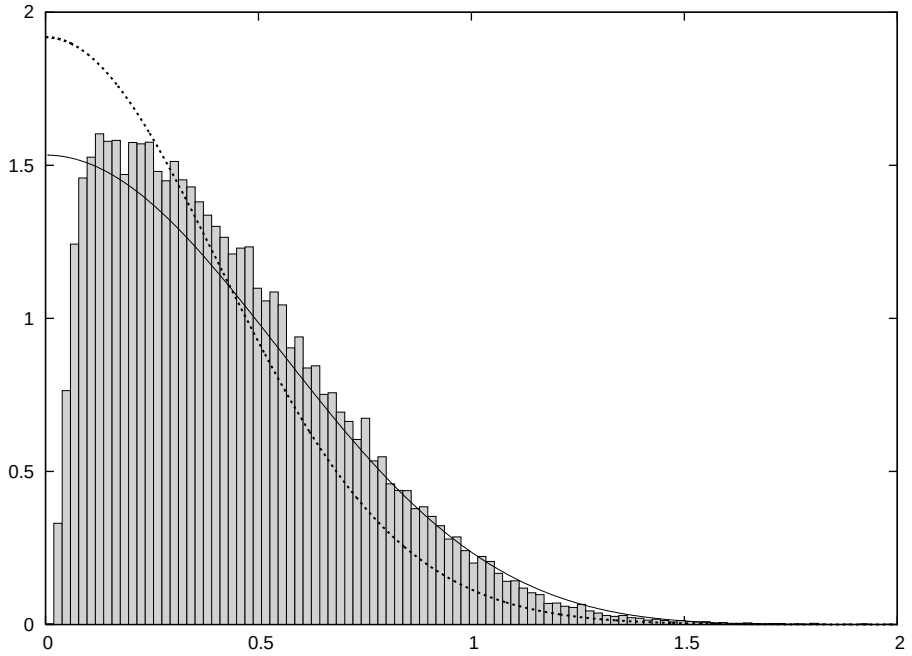

FIGURE 4. Distribution of the lowest zero for $L_{E_{11}}(s, \chi_d)$ with $0 < d \leq 400{,}000$ (bar chart), distribution of the lowest eigenvalue of $\mathrm{SO}(2N)$ with $N_{\text{eff}} = 2.14$ (solid), standard $N_{\text{std}} = 12.26$ (dots).

the lowest zero of each L-function in the family) is then depicted (for rank-zero curves) as a bar chart in figure 4 whereas the distribution of the lowest eigenvalue of $\mathrm{SO}(2N)$ with 'effective' matrix size N_{eff} is the solid curve and the one with 'standard' matrix size N_{std} is the dotted curve. The distribution of the lowest eigenvalue is related to the solution of a non-linear ordinary differential equation of Painlevé VI (see [23]). The curves for N_{eff} and N_{std} in figure 4 are computed for these non-integral values of N by establishing a numerical differential equation solver for Painlevé VI, which is developed in [20].

We observe from figure 4 that the distribution of the lowest eigenvalue of $\mathrm{SO}(2N_{\text{eff}})$ mimics the distribution of the lowest zero of rank-zero curves from $\mathcal{F}_E^+(X)$ much better both in the bulk and in the tail of the distribution than

$\mathrm{SO}(2N_{\mathrm{std}})$. However, near the origins we still find a large discrepancy. We address this discrepancy in the next section.

Substituting N_{eff} into (4.6) we obtain:

$$\frac{\pi}{N_{\mathrm{eff}}} R_1\left(\frac{\pi y}{N_{\mathrm{eff}}}\right) = \left(1+\frac{\sin(2\pi y)}{2\pi y}\right) - r_1\frac{1+\cos(2\pi y)}{L} - \frac{4r_1^2}{6}\frac{\pi y\sin(2\pi y)}{L^2} + O\left(\frac{1}{L^3}\right). \tag{4.11}$$

With the substitution $N = N_{\mathrm{eff}}$ the scaled one-level density of $\mathrm{SO}(2N)$ now agrees with our conjectural answer (4.2) for that of $\mathcal{F}_E^+(X)$ in the leading and next-to-leading order term. The method of Bogomolny *et al.* indicates how to proceed to find agreement down to the next order term of order L^{-2}. However, with our available data for twists up to $X = 400{,}000$ we are not working with sufficiently large X to proceed further with their method. For completeness, the details are worked out in [36].

5. Cut-off value for the excised ensemble

5.1. **Calculating the cut-off value.** We now develop an argument to determine the cut-off value c in (3.4). In [13] and [14], Conrey, Keating, Rubinstein and Snaith developed a method using random matrix theory to conjecture the asymptotic order of the number of L-functions in a family such as $\mathcal{F}_E^+(X)$ that vanish at the central point; alternatively, this is equivalent, on the Birch and Swinnerton-Dyer conjecture, to the asymptotic order of the number of curves of rank 2 or higher in the associated family of elliptic curves. Numerical tests support the prediction for the order, but the associated proportionality constant could not be determined. We will use numerical findings in those papers and the method introduced there to arrive at the cut-off value c.

We begin by reviewing the method of [13], modifying it to meet our current purpose. Adjusting slightly the notation of [13] to ours, let

$$M_E(X,s) = \frac{1}{X^*} \sum_{\substack{0<d\le X \\ L_E(s,\chi_d)\in\mathcal{F}_E^+(X)}} L_E(1/2,\chi_d)^s, \tag{5.1}$$

where $X^* = \#\{0 < d \le X \mid L_E(s,\chi_d) \in \mathcal{F}_E^+(X)\}$ is the number of terms in the sum above. Following the philosophy set out in [42] and [43] we expect that, for large X and $N \sim \log X$,

$$M_E(X,s) \sim a_s(E) M_O(N,s), \tag{5.2}$$

where

$$M_O(N,s) = \int_{SO(2N)} \Lambda_A(1,N)^s \, dA \tag{5.3}$$

and $a_s(E)$ is an arithmetical expression depending on the Dirichlet coefficients $\lambda(p)$ of the curve E:

$$\begin{aligned} a_s(E) = &\left[\prod_p \Big(1-\frac{1}{p}\Big)^{s(s-1)/2}\right] \\ &\times \left[\prod_{p\nmid M} \frac{p}{p+1}\left(\frac{1}{p}+\frac{1}{2}\Big[\mathcal{L}_p\Big(\frac{1}{p^{1/2}}\Big)^s+\mathcal{L}_p\Big(\frac{-1}{p^{1/2}}\Big)^s\Big]\right)\right] \\ &\times \mathcal{L}_M\Big(\frac{\pm\omega(E)}{M^{1/2}}\Big)^s. \end{aligned} \tag{5.4}$$

This holds for prime conductor M, where $\omega(E)$ is the sign of the functional equation of $L_E(s)$. For our purposes, the $\pm$ in the last line above must actually be $+$, corresponding to twists by *positive* fundamental discriminants $0 < d \le X$ (the $-$ sign corresponds to twists by negative fundamental discriminants $-X \le d < 0$). We define

$$\mathcal{L}_p(z) = \sum_n^{\infty} \lambda(p^n) z^n = (1-\lambda(p)z+\psi_M(p)z^2)^{-1}, \tag{5.5}$$

with $\psi_M(p)$ given at (2.5).

In (5.2), $M_O(N,s)$ denotes the moment generating function of the values $|\Lambda_A(1,N)|$ as A varies in the random matrix ensemble $\mathrm{SO}(2N)$ (the s^{th} moment is the expected value of $|\Lambda_A(1,N)|^s$). For $\mathrm{Re}(s) > -1/2$, $M_O(N,s)$ can be explicitly evaluated [43] as

$$M_O(N,s) = \int_{SO(2N)} \Lambda_A(1,N)^s\, dA = 2^{2Ns}\prod_{j=1}^{N}\frac{\Gamma(N+j-1)\Gamma(s+j-1/2)}{\Gamma(j-1/2)\Gamma(s+j+N-1)}. \tag{5.6}$$

Thus, from (5.6), we have information about the value distribution of the characteristic polynomials. More precisely, we have, for $c > 0$, that

$$P_O(N,x) = \frac{1}{2\pi i x}\int_{c-i\infty}^{c+i\infty} M_O(N,s)x^{-s}ds; \tag{5.7}$$

here $P_O(N,x)$ denotes the probability density for values of the characteristic polynomials $\Lambda_A(1,N)$ with $A \in \mathrm{SO}(2N)$.

For small $x > 0$, the regime of our interest, the major contribution in the integral on the right side of (5.7) comes from the simple pole at $s = -1/2$ in (5.6), thus

$$P_O(N,x) \sim x^{-1/2}h(N) \tag{5.8}$$

where

$$h(N) = \operatorname*{Res}_{s=-1/2} M_O(N,s) = 2^{-N}\Gamma(N)^{-1}\prod_{j=1}^{N}\frac{\Gamma(N+j-1)\Gamma(j)}{\Gamma(j-1/2)\Gamma(j+N-3/2)}. \tag{5.9}$$

We also make use, for large N, of the asymptotic

$$h(N) \sim 2^{-7/8}G(1/2)\pi^{-1/4}N^{3/8}, \tag{5.10}$$

where G is the Barnes G-function [2].

Notice that $P_O(N,x)\,dx$ is the probability that a characteristic polynomial $\Lambda_A(1,N)$ of $A \in SO(2N)$ takes a value between x and $x+dx$. Hence

$$\text{Prob}(0 \le \Lambda_A(1,N) \le \rho) = \int_0^\rho P_O(N,x)dx. \tag{5.11}$$

With (5.8) we have for small x that

$$\text{Prob}(0 \le \Lambda_A(1,N) \le \rho) \sim \int_0^\rho x^{-1/2}h(N)dx = 2\rho^{1/2}h(N). \tag{5.12}$$

We now define another probability density $P_E(d,x)$. Due to (5.2), we expect that this is in some sense a smooth approximation to the probability density for elliptic curve L-values from $\mathcal{F}_E^+(X)$ which have fundamental discriminants around d. We define, in analogy with (5.7),

$$P_E(d,x) := \frac{1}{2\pi i x}\int_{c-i\infty}^{c+i\infty} a_s(E)M_O(\log d, s)x^{-s}ds \sim a_{-1/2}(E)P_O(\log d, x). \tag{5.13}$$

The final approximation above holds for small x; it is obtained by shifting the line of integration left past the pole at $s=-1/2$ and picking up the respective residue of the integrand.

As described in section 3, the formula of Waldspurger *et al.* (2.7) implies a discretization of central L-values for elements from $\mathcal{F}_E^+(X)$ given by

$$L_E(1/2,\chi_d) = 0 \quad \text{whenever} \quad L_E(1/2,\chi_d) < \frac{\kappa_E}{\sqrt{d}}. \tag{5.14}$$

By calculating the probability that a random variable, Y_d, with probability density $P_E(d,x)$, takes a value less than $\kappa_E/\sqrt{d}$ and summing over d up to X, the authors in [13] and [14] predicted the correct order of magnitude for the number of L-functions that vanish at the central point (see Conjecture 5.1 of [14]). However, the constant factor could not be predicted correctly to agree with the numerical data. Since their cut-off value $\kappa_E/\sqrt{d}$ did not give the correct number of vanishing L-functions, we will presently work backwards and use the numerically calculated number of L-functions that are zero at the central point (numerical data from [14]) to deduce an "effective" cut-off $\frac{\delta\cdot\kappa_E}{\sqrt{d}}$ that *does* give the correct answer, for some $\delta > 0$. Thus we repeat the calculation of [13] but with the modified cut-off value.

We have

$$\begin{aligned}\text{Prob}\left(0 \le Y_d \le \frac{\delta\cdot\kappa_E}{\sqrt{d}}\right) &\sim \int_0^{\delta\kappa_E d^{-1/2}} a_{-1/2}(E)x^{-1/2}h(\log d)dx \\ &= 2a_{-1/2}(E)\left(\frac{\delta\cdot\kappa_E}{\sqrt{d}}\right)^{1/2} h(\log d).\end{aligned} \tag{5.15}$$

Now we follow [13] and conjecture that

$$\#\{L_E(s,\chi_d)\in\mathcal{F}_E^+(X), d \text{ prime} : L_E(1/2,\chi_d)=0\} = \sum_{\substack{d\le X\\ d \text{ prime}}}^{*} \text{Prob}\left(0\le Y_d\le \frac{\delta\kappa_E}{\sqrt{d}}\right)$$
$$\sim \frac{1}{4\log X}\sum_{n=1}^{\lfloor X\rfloor} 2a_{-1/2}(E)\left(\frac{\delta\kappa_E}{\sqrt{n}}\right)^{1/2} h(\log X), \quad (5.16)$$

where the starred sum means that d is restricted to *prime* fundamental discriminants for which $\chi_d(-M)\omega(E)=+1$ (of which, asymptotically, there are $X/(4\log X)$ of size at most X). Using (5.10), we get

$$\#\{L_E(s,\chi_d)\in\mathcal{F}_E^+(X), d \text{ prime} : L_E(1/2,\chi_d)=0\}$$
$$\sim \frac{1}{4\log X}\cdot 2\; a_{-1/2}(E)\sqrt{\kappa_E}\; 2^{-7/8}G(1/2)\pi^{-1/4}(\log X)^{3/8}\delta^{1/2}\cdot\tfrac{4}{3}X^{3/4}. \quad (5.17)$$

We wish to obtain a numerical value for δ. We would like to thank Michael Rubinstein for sharing his data from [14] on the number of L-functions that vanish at the central point. For a large number of elliptic curve families he computes the left side of (5.17) and divides it by

$$\frac{1}{4}a_{-1/2}(E)\sqrt{\kappa_E}X^{3/4}(\log X)^{-5/8}. \quad (5.18)$$

The results are plotted (see [14]) as a function of X; the curves flatten out and seem to approach a constant value. One such constant is:

$$0.2834620 \text{ for } E = 11A_r \quad (5.19)$$

where the nomenclature of the elliptic curve being twisted to form the family refers to Table 3 of [14]. We will refer to this family as twists of E_{11}.

Thus for twists of E_{11} we have

$$\tfrac{8}{3}2^{-7/8}G(1/2)\pi^{-1/4}\delta^{1/2}\approx 0.2834620. \quad (5.20)$$

With $G(1/2)$ evaluated as approximately 0.603244, we have

$$\delta\approx 0.185116. \quad (5.21)$$

For this family we have

$$\kappa_E = 6.346046521 \quad \text{and} \quad a_{-1/2}(E) = 0.732728078. \quad (5.22)$$

Thus, with δ given in (5.21) and κ_E in (5.22), we take the 'effective' cut-off to be

$$\delta\cdot\kappa_E = 1.17475. \quad (5.23)$$

That is, when modeling the distribution of L-values with $P_E(d,x)$, as described in [13], integrating up to the value of $\delta\kappa_E/\sqrt{d}$ gives the correct number of L-functions taking the value zero at the central point.

5.2. **Numerical evidence for the cut-off value: Standard $N_{\rm std}$.** The probability densities P_E and P_O are related, for small values of x (see (5.8) and (5.13)), by

$$P_E(d,x) \sim P_O\left(N_{\rm std}, a_{-1/2}^{-2}(E)x\right) \tag{5.24}$$

when $N_{\rm std} \sim \log d$. Thus a cut-off of $\delta\kappa_E/\sqrt{d}$ applied to $P_E(d,x)$ scales to

$$c_{\rm std} \times \exp(-N_{\rm std}/2) := a_{-1/2}^{-2}(E)\ \delta\ \kappa_E \times \exp(-N_{\rm std}/2) \tag{5.25}$$

for the distribution of values of characteristic polynomials of matrices of size $N_{\rm std}$. Substituting the numerical values we obtain

$$c_{\rm std} \approx 2.188. \tag{5.26}$$

We now present data using the standard matrix size $N_{\rm std}$ to model the zero statistics. Although we expect that the excised orthogonal ensemble models L-functions with discriminant around the value X, for numerical tests we take *all* $d \le X$ and set $N_{\rm std} \sim \log X$ so that we have a substantial data set.

As mentioned in section 4, and illustrated in figure 4, eigenvalues of $SO(2N)$ matrices with $N \sim \log X$ do not give particularly good agreement with the statistics of zeros of L-functions from $\mathcal{F}_E^+(X)$. The procedure of excising matrices with small values of $|\Lambda_A(1,N)|$ from the ensemble does not substantially change the bulk of the distribution. However, for E_{11}, we illustrate in figure 5 how we can scale the mean of the distribution of the first eigenvalue to obtain better agreement. The distribution of the first zero of even quadratic twists of $L_{E_{11}}(s)$ by prime discriminants between 0 and 400,000 has a mean of 0.4081. The distribution of the first eigenvalue of 3×10^6 matrices from $\mathrm{SO}(2N_{\rm std})$ conditioned to have $\Lambda_A(1,N_{\rm std}) \ge 2.188 \times \exp(-N_{\rm std}/2)$, with $N_{\rm std} = 12$ ($\approx \log(\sqrt{11}\ 400{,}000/2\pi)$) was found to be 0.365; deviation from the distribution of the first critical zero of the quadratic twists is quite visible, as illustrated in the left graphic of figure 5. Rescaling the random-matrix mean to match that of the L-function zeros gives the graphic on the right side of figure 5, showing much better agreement. The cumulative plot of the scaled distribution is shown in figure 6.

Working with the mean-scaled RMT results for $N = N_{\rm std}$, we test various values of c in (3.4). We measure the agreement with the zero distribution by averaging the absolute value of the difference between the cumulative distribution of the zeros and the cumulative distribution of the eigenvalues at a set of evenly spaced points (the blue crosses on figure 6). The plot of the difference between the cumulative distributions versus the cut-off parameter is shown in figure 7, where c varies along the horizontal axis. We see a minimum at $c_{\rm std} = 2.188$; this is the value predicted in section 5.1 and is marked with a dotted vertical line.

Initially we thought that an equally plausible way to calculate a cut-off value would be to equate not the probability densities, as in (5.24), but rather the probability of finding an L-value of zero with the probability of discarding a random matrix on the basis of the condition (3.4). Equating probabilities would lead to a

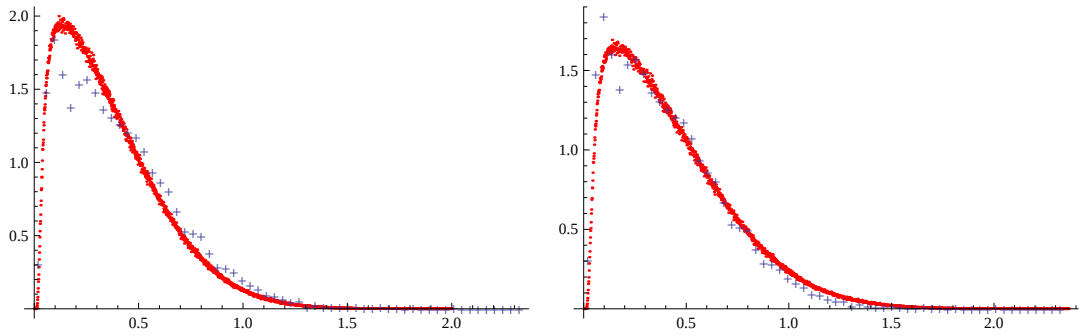

FIGURE 5. Probability density of the first eigenvalue from 3×10^6 numerically generated matrices $A \in SO(2N_{\text{std}})$ with $|\Lambda_A(1, N_{\text{std}})| \geq 2.188 \times \exp(-N_{\text{std}}/2)$ and $N_{\text{std}} = 12$ (red dots) compared with the first zero of even quadratic twists $L_{E_{11}}(s, \chi_d)$ with prime fundamental discriminants $0 < d \leq 400{,}000$ (blue crosses). In the left picture the random matrix data is not scaled, in the picture on the right the mean of the distribution is scaled to match that of the zero data.

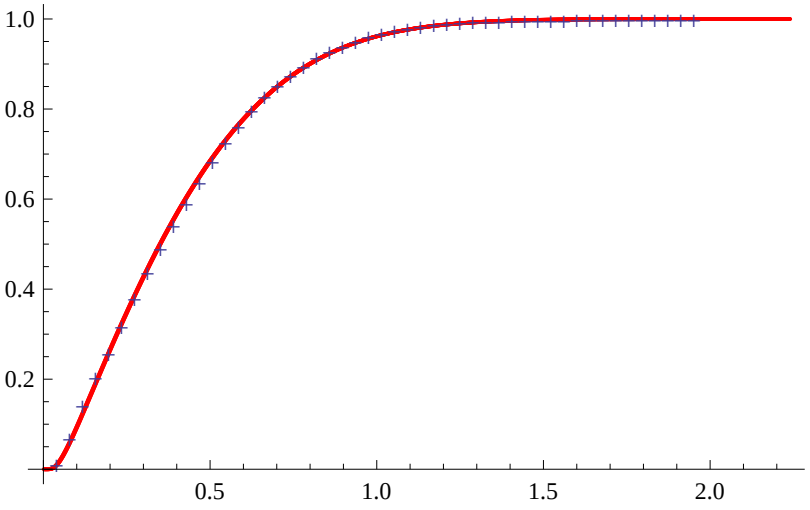

FIGURE 6. Cumulative probability density of the first eigenvalue from 3×10^6 numerically generated matrices $A \in SO(2N_{\text{std}})$ with $|\Lambda_A(1, N_{\text{std}})| \geq 2.188 \times \exp(-N_{\text{std}}/2)$ and $N_{\text{std}} = 12$ (red dots) compared with the first zero of even quadratic twists $L_{E_{11}}(s, \chi_d)$ with prime fundamental discriminants $0 < d \leq 400{,}000$ (blue crosses). The random matrix data is scaled so that the means of the two distributions agree.

calculation such as

$$\begin{aligned}\int_0^{\delta\kappa_E/\sqrt{d}} P_E(d,x)dx &\sim \int_0^{\delta\kappa_E/\sqrt{d}} a_{-1/2}(E)x^{-1/2}h(\log d)\,dx \\ &= \int_0^{a_{-1/2}^2(E)\delta\kappa_E/\sqrt{d}} y^{-1/2}h(N_{\text{std}})\,dy \\ &\sim \int_0^{a_{-1/2}^2(E)\delta\kappa_E/\sqrt{d}} P_O(N_{\text{std}},y)\,dy,\end{aligned} \tag{5.27}$$

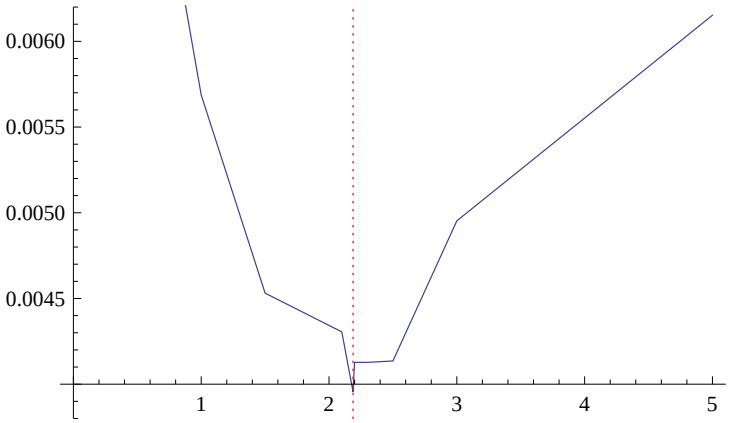

FIGURE 7. A measure of the difference between the mean-scaled cumulative distribution of the first eigenvalue of the excised random matrix model (5.26) with $N_{\text{std}} = 12$ for various values of c and the cumulative distribution of the first zero of even quadratic twists $L_{E_{11}}(s, \chi_d)$ with prime fundamental discriminants $0 < d \leq 400{,}000$. The values $c_{\text{std}} = 2.188$ is marked with a vertical line.

implying a cut-off of

$$a_{-1/2}^2(E)\delta\kappa_E \exp(-N_{\text{std}}/2) \approx 0.6307 \exp(-N_{\text{std}}/2). \tag{5.28}$$

From figure 7 we see that $c = 0.6307$ certainly does not minimize the error between the excised random matrix model and the zero statistics.

It is noteworthy that matching probability densities, rather than probabilities, appears to be the correct model. Taking the cut-off value c_{std} that best models the zero data (as calculated at the beginning of this section by matching densities) means that the proportion of the matrices that are being excluded by the condition (3.4) is not the same as the proportion of L-functions from our family of quadratic twists that are excluded from the zero statistics because they have rank higher than zero. The reason for this, and whether the excluded matrices might potentially model the L-functions associated with the higher-rank curves, are topics for future investigation.

5.3. **Numerical evidence for the cut-off value: N_{eff}.** The excised model can be applied using orthogonal matrices of any even size $2N$. We will presently use a method identical to that in the previous section; however, now we find the cut-off for matrices of size $N = N_{\text{eff}}$ (which was calculated in section 4). We recall the shape of $P_O(N, x)$ for small x and large N, equations (5.8) and (5.10), and see

$$\begin{aligned} P_E(d, x) \sim a_{-1/2}x^{-1/2}h(\log d) &\sim a_{-1/2}x^{-1/2}h(2r_1N_{\text{eff}}) \\ &\sim a_{-1/2}x^{-1/2}(2r_1)^{3/8}h(N_{\text{eff}}) \\ &\sim P_O\left(N_{\text{eff}}, a_{-1/2}^{-2}(E)\ (2r_1)^{-3/4}x\right). \end{aligned} \tag{5.29}$$

Thus a cut-off of $\delta\kappa_E/\sqrt{d}$ applied to $P_E(d, x)$ scales to

$$c_{\text{eff}} \times \exp(-N_{\text{std}}/2) := a_{-1/2}^{-2}(E)(2r_1)^{-3/4}\ \delta\ \kappa_E \times \exp(-r_1N_{\text{eff}}) \tag{5.30}$$

for the distribution of values of characteristic polynomials of matrices of size N_{eff}. Plugging in the numerical values we obtain, with $r_1 = 2.8600$ for E_{11} (given at (4.8))

$$c_{\text{eff}} \approx 0.5916. \tag{5.31}$$

For this matrix size we use the cut-off value $c = c_{\text{eff}}$ in (3.4).

We now compare data for zeros of elliptic curve L-functions to matrices of size N_{eff}.

We note here that, although the most accurate description of our expectation is that the excised orthogonal ensemble models L-functions with discriminant around the value d when $N_{\text{eff}} \sim \log d/(2r_1)$, for numerical tests we take all d in an interval such as $0 < d \leq X$ and set $N_{\text{eff}} \sim \log X/(2r_1)$. This is the most effective way to acquire enough data to have good resolution in the plots.

For E_{11} we have computed zeros of *even* twists $L_{E_{11}}(s, \chi_d)$ for prime d between 0 and 400,000 which do *not* vanish at the central point. We compare the distribution of the first zero above the critical point of these L-functions with the numerically generated distribution of first eigenvalues of 3×10^6 matrices from the excised ensemble SO(4) (in section 4 we computed $N_{\text{eff}} = 2.14$) for various values of the cut-off c. Figure 8 shows the probability density and the cumulative probability density of first zeros and eigenvalues for $c_{\text{eff}} = 0.5916$. In contrast to modeling with matrices of size N_{std}, here we do *not* scale the mean of the distribution; however, for those interested, we note that the probability density of the zeros has mean 0.4081 and the probability density of the eigenvalues has mean 0.4234.

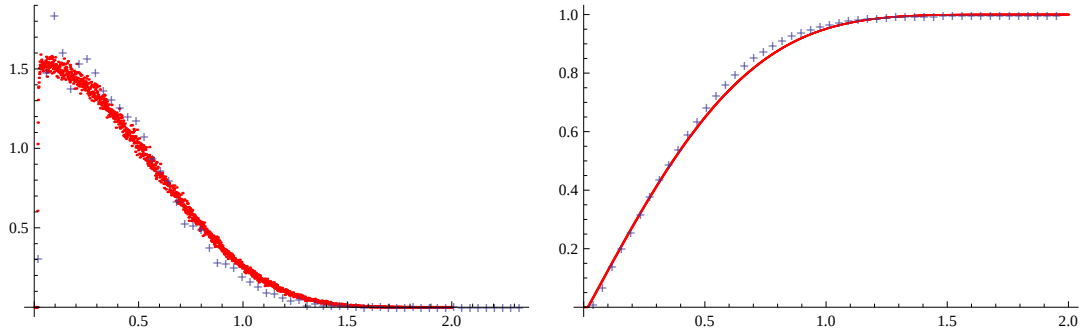

FIGURE 8. Probability density (left) and cumulative probability density (right) of the first eigenvalue from 3×10^6 numerically generated matrices $A \in SO(2N_{\text{eff}})$ with $|\Lambda_A(1, N_{\text{eff}})| \geq 0.5916 \times \exp(-r_1 N_{\text{eff}})$ and $N_{\text{eff}} = 2$ (red dots) compared with the first zero of rank zero even quadratic twists $L_{E_{11}}(s, \chi_d)$ with prime fundamental discriminants $0 < d \leq 400{,}000$ (blue crosses).

In figure 9 we plot a measure of the difference between the first zero distribution and the distribution of the first eigenvalue for various values of the cut-off c. Here the error is calculated by summing the absolute value of the difference between the cumulative distribution of the zeros and the cumulative distribution of the eigenvalues at a set of evenly spaced points (the positions of the blue crosses in figure 8) and dividing by the number of points. We see a minimum at $c_{\text{eff}} = 0.5916$; this is the value predicted in section 5.1 and is marked with a dotted vertical line.

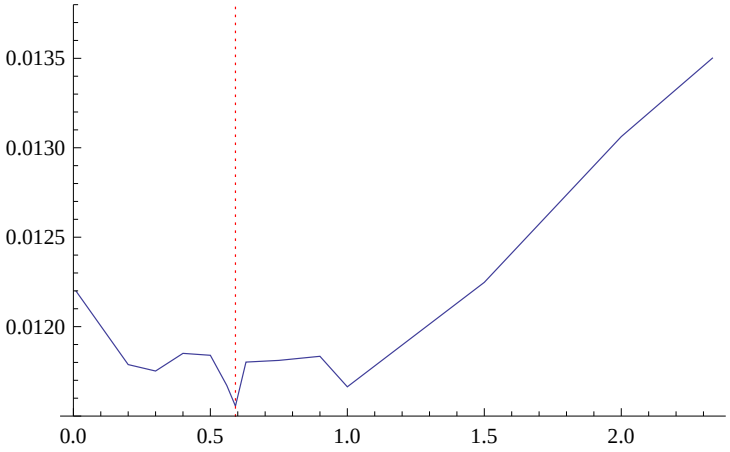

FIGURE 9. A measure of the difference between the cumulative distribution of the first eigenvalue of the excised random matrix model (3.4), as c varies along the horizontal axis, and the cumulative distribution of the first zero of rank zero even quadratic twists $L_{E_{11}}(s, \chi_d)$ of with prime fundamental discriminants $0 < d \leq 400{,}000$. The value $c_{\text{eff}} = 0.5916$ is marked with a vertical line.

As in the previous section, another possible model is to equate probabilities rather than probability densities. For N_{eff} this leads to

$$c = (2r_1)^{3/4} a^2_{-1/2}(E)\delta\kappa_E \approx 2.3328. \tag{5.32}$$

Again, from figure 9 we see that this does not come close to minimizing the error.

5.4. **Excised model and the one-level density.** In section 4 we provided evidence that the lower-order terms of the one-level density of $\mathcal{F}_E^+(X)$ determine an effective matrix size N_{eff} such that the distribution of first eigenvalues of $\mathrm{SO}(2N_{\text{eff}})$ models the bulk and tail of the distribution of first zeros of $\mathcal{F}_E^+(X)$. In sections 5.1–5.3 we discussed how to obtain an appropriate cut-off value for the characteristic polynomial Λ_A at 1 with $A \in \mathrm{SO}(2N)$ so that the distribution of first eigenvalues of this subset of $\mathrm{SO}(2N)$ models the region at and near the origin of the distribution of first zeros of $\mathcal{F}_E^+(X)$. Here the matrix size is either the effective one, i.e., $N = N_{\text{eff}}$ or the standard one, i.e., $N = N_{\text{std}}$. In the first case no further scaling is undertaken whereas in the latter one we match mean densities of $\mathrm{SO}(2N_{\text{std}})$ to $\mathcal{F}_E^+(X)$ to achieve qualitative and quantitative agreement throughout the origin, bulk and tail between the cumulative distribution of first eigenvalues of $\mathrm{SO}(2N)$ and cumulative distribution of first zeros of $\mathcal{F}_E^+(X)$. In this section we explore to what extent the values for the matrix size and the cut-off value on the characteristic polynomial used for the distribution of first eigenvalues (to model the distribution of first zeros) can be applied to the one-level density of eigenvalues (to model the one-level density of zeros). We compare zero data of the family $\mathcal{F}_E^+(X)$ of quadratic twists $L_{E_{11}}(s, \chi_d)$ with prime fundamental discriminants $0 < d < X = 400,000$ to eigenvalue statistics of random matrices from $\mathrm{SO}(2N)$ for two values of N. Figure 10 depicts as a red solid line the one-level density of matrices A from $\mathrm{SO}(2N_{\text{std}})$ with characteristic polynomials constrained to obey

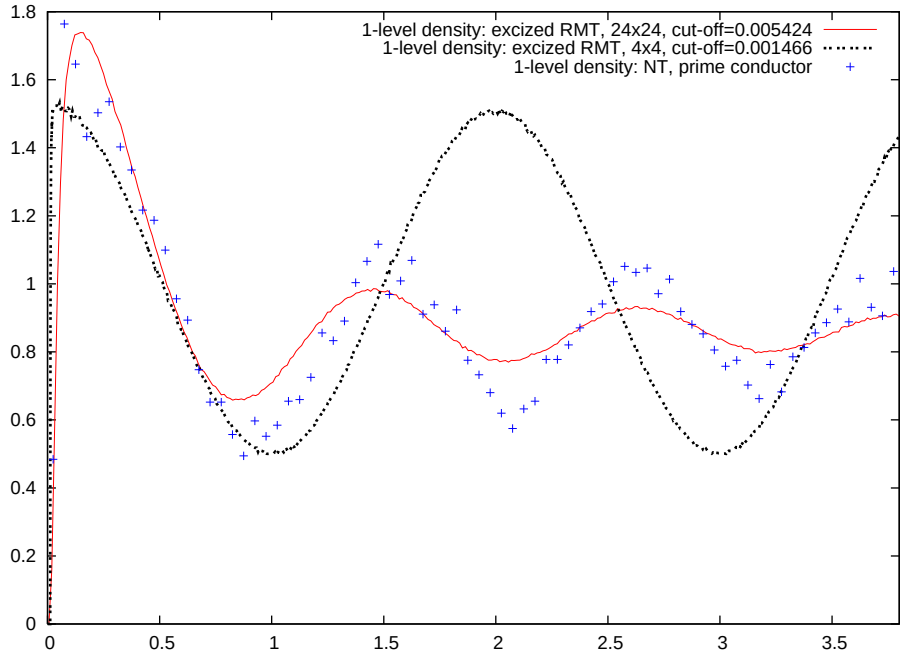

FIGURE 10. *Red solid line:* One-level density of 9.12×10^6 numerically generated matrices from $\mathrm{SO}(2N_{\mathrm{std}})$ and cut-off $|\Lambda_A(1, N_{\mathrm{std}})| \geq 2.188 \times \exp(-N_{\mathrm{std}}/2) = 0.005424$, scaled so that the mean of the first eigenvalue matches that of the first zero. *Black dotted line:* One-level density of 9.8×10^6 numerically generated matrices from $\mathrm{SO}(2N_{\mathrm{eff}})$ and cut-off $|\Lambda_A(1, N_{\mathrm{eff}})| \geq 0.5916 \times \exp(-N_{\mathrm{std}}/2) = 0.001466$. *Blue crosses:* One-level density for zeros of even quadratic twists $L_{E_{11}}(s, \chi_d)$ with prime fundamental discriminant between 0 and 400,000.

$|\Lambda_A(1, N_{\mathrm{std}})| \geq 2.188 \times \exp(-N_{\mathrm{std}}/2) = 0.005424$ with $N_{\mathrm{std}} = 12$. We obtained this by generating 9.12×10^6 matrices from $\mathrm{SO}(24)$. This one-level density on the random matrix theory (RMT) side has been scaled, in the horizontal direction, with the scaling factor $0.4081/0.365 = 1.118$ which we obtained numerically when comparing with the distribution of the first zeros in section 5.2. The one-level density of matrices A from $\mathrm{SO}(2N_{\mathrm{eff}})$ with $N_{\mathrm{eff}} = 2$ where the characteristic polynomials are constrained to obey $|\Lambda_A(1, N_{\mathrm{eff}})| \geq 0.5916 \times \exp(-N_{\mathrm{std}}/2) = 0.001466$ is depicted as a dotted line. We obtained this by generating 9.8×10^6 matrices from $\mathrm{SO}(4)$. No scaling of means has been undertaken in this case. The one-level density for zeros of rank-zero, even quadratic twists of E_{11} with prime discriminant between 0 and 400 000 is depicted as blue crosses. In the N_{std} case we find correlation with the zero data over a wide range whereas in the N_{eff} case we only find some agreement up to the first unit mean spacing. Thereafter we see a clear discrepancy.

In figure 11 we consider the associated cumulative distributions from figure 10. Here we observe that the distributions of N_{std} (red line) and the zero data (blue

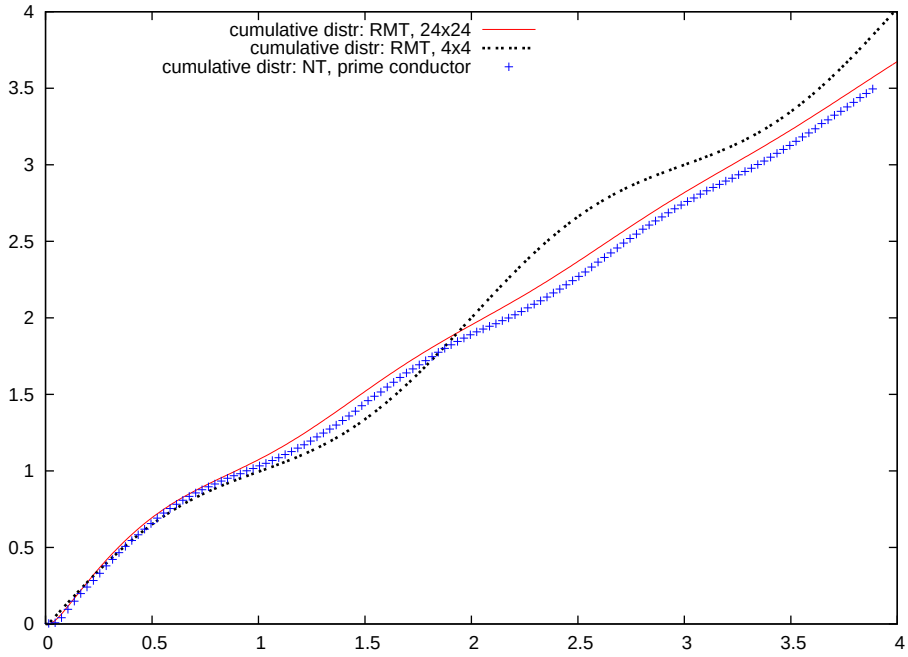

FIGURE 11. Cumulative distributions of one-level densities from figure 10. *Red solid line:* numerically generated matrices from $\mathrm{SO}(2N_{\mathrm{std}})$, with scaling; *dotted line:* numerically generated matrices from $\mathrm{SO}(2N_{\mathrm{eff}})$; *blue crosses:* zeros of even quadratic twists $L_{E_{11}}(s, \chi_d)$ with prime fundamental discriminants between 0 and 400,000.

crosses) track each other over a wide range, whereas the distributions of N_{eff} (dotted line) and the zero data (blue crosses) track each other only up to the first unit spacing. Thereafter the behaviour of the zeros is not captured.

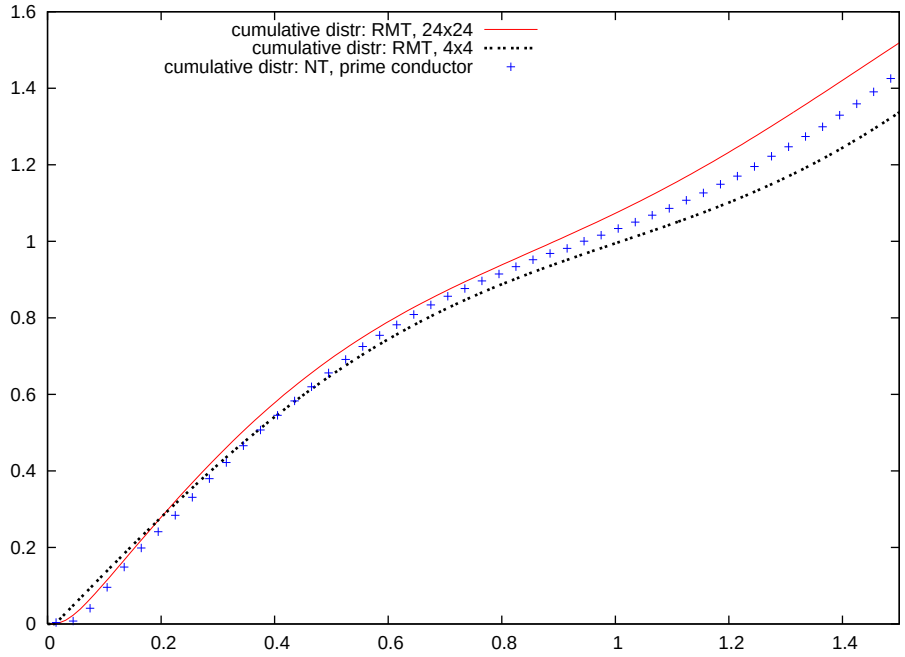

FIGURE 12. Magnification of figure 11, i.e., cumulative distributions of one-level densities from figure 10. *Red solid line:* numerically generated matrices from $\mathrm{SO}(2N_{\mathrm{std}})$, with scaling; *dotted line:* numerically generated matrices from $\mathrm{SO}(2N_{\mathrm{eff}})$; *blue crosses:* zeros of even quadratic twists $L_{E_{11}}(s, \chi_d)$ with prime conductor between 0 and 400,000.

Figure 12 is a magnification of figure 11. Here we observe that also the slope of the zero data near the origin is nicely captured by the excised RMT model with standard matrix size N_{std}. This feature is not so clear in the N_{eff} case.

In summary, to answer the question to what extent the values for the matrix size and the cut-off value of the characteristic polynomial used to model the distribution of first zeros by the distribution of first eigenvalues can be applied to the one-level density, we find that we achieve better agreement when choosing the excised ensemble with standard matrix size (with the data scaled so that the mean value of the first eigenvalue matches that of the first zero) than choosing the excised ensemble with effective matrix size. In the latter case we only obtain agreement up to the first unit mean spacing and in the former we get agreement over a wide range. It should be noted here that we only require our model to give useful predictions over a distance of one mean spacing, because further from the origin we know from [37] that the one level density is strongly dominated by arithmetic contributions that are accurately modelled by methods directly incorporating number theoretical information.

6. One-level density for the excised random matrix model

In the previous sections we provided evidence that we can use eigenvalue statistics of random matrices from the excised orthogonal ensemble to model the zero statistics for the family $\mathcal{F}_E^+(X)$ of even quadratic twists of a fixed elliptic curve L-function. Our goal in this section is to compute the one-level density $R_1^{T_{\mathcal{X}}}$ for $T_{\mathcal{X}}$, the ensemble defined in the introduction. The main results are contained in the three theorems set out in the introduction. We prove those theorems in this section.

6.1. **Proof of Theorem 1.1.**

Proof. Consider

$$R_1^{T_{\mathcal{X}}}(\theta_1) := C_{\mathcal{X}} \cdot N \int_0^{\pi} \cdots \int_0^{\pi} H(\log|\Lambda_A(1,N)| - \mathcal{X}) \times \\ \times \prod_{j<k} (\cos\theta_j - \cos\theta_k)^2 d\theta_2 \cdots d\theta_N, \quad (6.1)$$

which is the one-level density for the set $T_{\mathcal{X}}$. Here $H(x)$ denotes the Heaviside function

$$H(x) = \begin{cases} 1 \text{ for } x > 0 \\ 0 \text{ for } x < 0, \end{cases} \quad (6.2)$$

and $C_{\mathcal{X}}$ is a normalization constant (which we discuss later). Next, we replace in (6.1) the Heaviside function with its integral representation

$$H(x) = \frac{1}{2\pi i} \int_{c-i\infty}^{c+i\infty} \frac{\exp(rx)}{r} dr, \quad (6.3)$$

where $c > 0$, and observe that

$$\begin{aligned} \Lambda_A(1,N) = \Lambda_A(\exp(i\theta),N)\Big|_{\theta=0} &= \prod_{j=1}^{N} (1-\exp(i\theta_j))(1-\exp(-i\theta_j)) \\ &= 2^N \prod_{j=1}^{N} (1-\cos\theta_j). \end{aligned} \quad (6.4)$$

Thus, we have

$$H(\log|\Lambda_A(1,N)| - \mathcal{X}) = \frac{1}{2\pi i} \int_{c-i\infty}^{c+i\infty} 2^{Nr} \frac{\exp(-r\mathcal{X})}{r} \prod_{j=1}^{N} (1-\cos\theta_j)^r dr. \quad (6.5)$$

Substituting (6.5) into (6.1) gives

$$R_1^{T_{\mathcal{X}}}(\theta_1) = \frac{C_{\mathcal{X}}}{2\pi i} \int_{c-i\infty}^{c+i\infty} 2^{Nr} \frac{\exp(-r\mathcal{X})}{r} \, N \int_0^{\pi} \cdots \int_0^{\pi} \prod_{j=1}^{N} (1-\cos\theta_j)^r \times \\ \times \prod_{j<k} (\cos\theta_j - \cos\theta_k)^2 d\theta_2 \cdots d\theta_N \, dr. \quad (6.6)$$

Now, observe that in (6.6) we have

$$N\int_0^\pi\cdots\int_0^\pi\prod_{j=1}^N(1-\cos\theta_j)^r\prod_{j<k}(\cos\theta_j-\cos\theta_k)^2d\theta_2\cdots d\theta_N$$
$$=N\int_0^\pi\cdots\int_0^\pi\prod_{j=1}^N w^{(r-1/2,-1/2)}(\cos\theta_j)\prod_{j<k}(\cos\theta_j-\cos\theta_k)^2d\theta_2\cdots d\theta_N \quad (6.7)$$

where $w^{(\alpha,\beta)}(\cos\theta)=(1-\cos\theta)^{\alpha+1/2}(1+\cos\theta)^{\beta+1/2}$ is the weight function for the Jacobi ensemble of random matrices [24]. We now observe that

$$R_1^{J_N}(\theta_1;\alpha,\beta)=\int_0^\pi\cdots\int_0^\pi\prod_{j=1}^N w^{(r-1/2,-1/2)}(\cos\theta_j)\prod_{j<k}(\cos\theta_j-\cos\theta_k)^2d\theta_2\cdots d\theta_N \quad (6.8)$$

is the one-level density for the Jacobi ensemble J_N. This completes the proof. □

6.2. **Computation of the normalization constant $C_{\mathcal{X}}$.** Recall that when integrating over $\mathrm{SO}(2N)$ with respect to the normalized Haar measure using Weyl's integration formula [61] the normalization constant $C_{\mathrm{SO}(2N)}$ is determined by

$$1=\int_{\mathrm{SO}(2N)}dA=C_{\mathrm{SO}(2N)}\int_{[0,\pi]^N}\prod_{j<k}(\cos\theta_j-\cos\theta_k)^2d\theta_1\cdots d\theta_N. \quad (6.9)$$

Selberg's integral formula states that for integral N and complex r,s with $\mathrm{Re}(r)$, $\mathrm{Re}(s)>-1/2$

$$\int_0^\pi d\phi_1\cdots\int_0^\pi d\phi_N\prod_{l=1}^N(1-\cos\phi_l)^r(1+\cos\phi_l)^s\prod_{1\le j<k\le N}(\cos\phi_j-\cos\phi_k)^2$$
$$=2^{N(N+r+s-1)}\times\prod_{j=0}^{N-1}\frac{\Gamma(2+j)\Gamma(s+1/2+j)\Gamma(r+1/2+j)}{\Gamma(s+r+N+j)}. \quad (6.10)$$

Using (6.10) the normalization constant has the explicit form

$$C_{\mathrm{SO}(2N)}=2^{-N(N-1)}\prod_{j=0}^{N-1}\frac{\Gamma(N+j)}{\Gamma(2+j)\Gamma(1/2+j)^2}. \quad (6.11)$$

Likewise, the normalization constant $C_{\mathcal{X}}$ is determined by

$$1=C_{\mathcal{X}}\int_{[0,\pi]^N}H(\log\Lambda_A(1,N)-\mathcal{X})\prod_{j<k}(\cos\theta_j-\cos\theta_k)^2d\theta_1\cdots d\theta_N. \quad (6.12)$$

Using (6.5) yields

$$\frac{C_{\mathrm{SO}(2N)}}{C_{\mathcal{X}}}=\frac{C_{\mathrm{SO}(2N)}}{2\pi i}\int_{c-i\infty}^{c+i\infty}\int_{[0,\pi]^N}d\theta_1\cdots d\theta_N d\alpha\times$$
$$\times 2^{N\alpha}\frac{\exp(-\alpha\mathcal{X})}{\alpha}\prod_{j=1}^N(1-\cos\theta_j)^\alpha\prod_{j<k}(\cos\theta_j-\cos\theta_k)^2. \quad (6.13)$$

Substituting (6.11) into (6.13) and applying Selberg's integral formula (6.10) we obtain

$$\frac{C_{\mathrm{SO}(2N)}}{C_{\mathcal{X}}} = \frac{1}{2\pi i}\int_{c-i\infty}^{c+i\infty} \frac{\exp(-\alpha\mathcal{X})}{\alpha} 2^{2N\alpha} \prod_{j=0}^{N-1} \frac{\Gamma(N+j)\Gamma(\alpha+1/2+j)}{\Gamma(\alpha+N+j)\Gamma(1/2+j)} d\alpha. \quad (6.14)$$

The evaluation of (6.14) boils down to closing the contour to the left and to computing the residues associated to the poles at $\alpha = 0$ and the negative half integers coming from the $\Gamma(\alpha + 1/2 + j)$-term. The residue at the simple pole $\alpha = 0$ is 1 and the residue at the simple pole at $\alpha = -1/2$ is

$$-2\exp(\mathcal{X}/2)2^{-N}\frac{\Gamma(N)}{\Gamma(N-1/2)\Gamma(1/2)} \prod_{j=1}^{N-1} \frac{\Gamma(N+j)\Gamma(j)}{\Gamma(N+j-1/2)\Gamma(1/2+j)}. \quad (6.15)$$

We denote the contribution to (6.14) from residues of higher order poles at $\alpha_k = \frac{-1-2k}{2}$ with $k = 1, 2, 3, \ldots$ by

$$\sum_{k\geq 1} a_k \exp((k+1/2)\chi). \quad (6.16)$$

Thus, we obtain

$$\begin{aligned}\frac{C_{\mathrm{SO}(2N)}}{C_{\mathcal{X}}} = 1 &- \frac{\exp(\mathcal{X}/2)}{2^{N-1}}\frac{\Gamma(N)}{\Gamma(N-1/2)\Gamma(1/2)} \prod_{j=1}^{N-1} \frac{\Gamma(N+j)\Gamma(j)}{\Gamma(N+j-1/2)\Gamma(1/2+j)} \\ &+ \sum_{k\geq 1} a_k \exp((k+1/2)\chi).\end{aligned} \quad (6.17)$$

Notice that when $\mathcal{X} \to -\infty$ we have $C_{\mathcal{X}} \to C_{\mathrm{SO}(2N)}$, as expected. The regime of interest for us is when $\mathcal{X} < 0$. From (6.16) we see that the contributions of residues of higher poles decrease exponentially for $\mathcal{X} < 0$. The computation of residues of higher order poles is easily done with a computer algebra system (we used Mathematica). We find that for reasonable $\mathcal{X}$ we have good convergence using about 10 poles. When using only the K rightmost poles the error term is $O(\exp(-c_K\mathcal{X}))$ with $\alpha_{K+1} < c_K < \alpha_K$. We refer to section 6.4 for the relevant details. There we will also discuss the convergence of a series similar to (6.16). We are then left to show that the contribution from closing the contour is 0. This is indeed the case for $\exp(\mathcal{X}) < 2^{2N} = \max[\Lambda_A(1, N)]$ but we skip the calculation here and instead also refer to section 6.4 as we do a similar computation for $R_1^{T_{\mathcal{X}}}$ there.

6.3. **Proof of Theorem 1.2.**

Proof. We rewrite (6.6) so we can apply standard methods in the theory of orthogonal polynomials. First we consider the general Jacobi ensemble with weight function $(1-x)^\alpha(1+x)^\beta$ and then specialize to our setting with $\alpha = r - 1/2$ and $\beta = -1/2$. Notice that the weight function here differs slightly from the one in section 1.

Following Szegő [59] we define the Jacobi polynomials $P_n^{(\alpha,\beta)}(x)$, $\alpha, \beta > -1$, which satisfy

$$\int_{-1}^{1} P_n^{(\alpha,\beta)}(x) P_m^{(\alpha,\beta)}(x)(1-x)^\alpha (1+x)^\beta dx = \delta_{nm} h_n^{(\alpha,\beta)}, \tag{6.18}$$

where

$$h_n^{(\alpha,\beta)} = \frac{2^{\alpha+\beta+1}}{2n+\alpha+\beta+1} \frac{\Gamma(n+\alpha+1)\Gamma(n+\beta+1)}{\Gamma(n+1)\Gamma(n+\alpha+\beta+1)}. \tag{6.19}$$

Changing to angular variables, (6.18) takes the equivalent form

$$\int_0^\pi P_n^{(\alpha,\beta)}(\cos\theta) P_m^{(\alpha,\beta)}(\cos\theta)(1-\cos\theta)^{\alpha+1/2}(1+\cos\theta)^{\beta+1/2} d\theta = \delta_{nm} h_n^{(\alpha,\beta)}. \tag{6.20}$$

Using the Vandermonde determinant and further matrix row and column operations we have

$$\begin{aligned}
\prod_{j<k}(\cos\theta_k - \cos\theta_j) &= \begin{vmatrix} 1 & \cos\theta_1 & \cos^2\theta_1 & \dots & \cos^{N-1}\theta_1 \\ 1 & \cos\theta_2 & \cos^2\theta_2 & \dots & \cos^{N-1}\theta_2 \\ \vdots & \vdots & \vdots & \ddots & \vdots \\ 1 & \cos\theta_N & \cos^2\theta_N & \dots & \cos^{N-1}\theta_N \end{vmatrix} \\
&= \prod_{j=0}^{N-1} \frac{(h_j^{(\alpha,\beta)})^{1/2}}{\ell_j^{(\alpha,\beta)}} \times \\
&\times \begin{vmatrix} \frac{1}{\sqrt{h_0^{(\alpha,\beta)}}} P_0^{(\alpha,\beta)}(\cos\theta_1) & \frac{1}{\sqrt{h_1^{(\alpha,\beta)}}} P_1^{(\alpha,\beta)}(\cos\theta_1) & \dots & \frac{1}{\sqrt{h_{N-1}^{(\alpha,\beta)}}} P_{N-1}^{(\alpha,\beta)}(\cos\theta_1) \\ \frac{1}{\sqrt{h_0^{(\alpha,\beta)}}} P_0^{(\alpha,\beta)}(\cos\theta_2) & \frac{1}{\sqrt{h_1^{(\alpha,\beta)}}} P_1^{(\alpha,\beta)}(\cos\theta_2) & \dots & \frac{1}{\sqrt{h_{N-1}^{(\alpha,\beta)}}} P_{N-1}^{(\alpha,\beta)}(\cos\theta_2) \\ \vdots & \vdots & \ddots & \vdots \\ \frac{1}{\sqrt{h_0^{(\alpha,\beta)}}} P_0^{(\alpha,\beta)}(\cos\theta_N) & \frac{1}{\sqrt{h_1^{(\alpha,\beta)}}} P_1^{(\alpha,\beta)}(\cos\theta_N) & \dots & \frac{1}{\sqrt{h_{N-1}^{(\alpha,\beta)}}} P_{N-1}^{(\alpha,\beta)}(\cos\theta_N) \end{vmatrix},
\end{aligned} \tag{6.21}$$

where $\ell_j^{(\alpha,\beta)}$ is the leading coefficient of the polynomial $P_j^{(\alpha,\beta)}$:

$$\ell_j^{(\alpha,\beta)} = 2^{-j} \binom{2j+\alpha+\beta}{j}. \tag{6.22}$$

Thus we have the following determinantal expression

$$\begin{aligned}
&\prod_{j<k}(\cos\theta_k - \cos\theta_j)^2 \\
&= \prod_{j=0}^{N-1} \frac{h_j^{(\alpha,\beta)}}{(\ell_j^{(\alpha,\beta)})^2} \det\left(\sum_{n=1}^{N} (h_{n-1}^{(\alpha,\beta)})^{-1} P_{n-1}^{(\alpha,\beta)}(\cos\theta_j) P_{n-1}^{(\alpha,\beta)}(\cos\theta_k) \right)_{j,k=1,\dots,N}.
\end{aligned} \tag{6.23}$$

Setting

$$C_{s,r} := 2^{-N(N+r+s-1)} \prod_{j=0}^{N-1} \frac{\Gamma(s+r+N+j)}{\Gamma(2+j)\Gamma(s+1/2+j)\Gamma(r+1/2+j)}, \tag{6.24}$$

the normalized measure is

$$\begin{aligned}
&C_{s,r}\prod_{j=1}^{N}(1-\cos\theta_j)^r(1+\cos\theta_j)^s\prod_{j<k}(\cos\theta_k-\cos\theta_j)^2\\
&=\frac{1}{N!}\det\Big(\big(\sum_{n=1}^{N}(h_{n-1}^{(r-1/2,s-1/2)})^{-1}P_{n-1}^{(r-1/2,s-1/2)}(\cos\theta_j)P_{n-1}^{(r-1/2,s-1/2)}(\cos\theta_k)\big)\times\\
&\qquad\qquad\times(1+\cos\theta_j)^{s/2}(1-\cos\theta_j)^{r/2}(1+\cos\theta_k)^{s/2}(1-\cos\theta_k)^{r/2}\Big)_{j,k=1,\dots,N}\\
&=\frac{1}{N!}\det\Big(f_N^{(r-1/2,s-1/2)}(\theta_j,\theta_k)\Big)_{j,k=1,\dots,N},
\end{aligned}\tag{6.25}$$

where $f_N^{(r-1/2,s-1/2)}(\theta_j,\theta_k)$ is implicitly defined as the expression inside 'det(·)' in the middle term above.

Observe that this determinantal kernel f_N satisfies the hypotheses of Gaudin's Lemma (see e.g. Theorem 5.2.1 in [46]), namely

$$\int_0^\pi f_N^{(r-1/2,s-1/2)}(\theta,\theta)d\theta=N\tag{6.26}$$

and

$$\int_0^\pi f_N(x,\theta)f_N(\theta,y)d\theta=f_N(x,y).\tag{6.27}$$

By Gaudin's Lemma we then have

$$\int_0^\pi\det(f(\theta_j,\theta_k))_{j,k=1,\dots,N}d\theta_N=(N-(N-1))\det(f(\theta_j,\theta_k))_{j,k=1,\dots,N-1}.\tag{6.28}$$

Applying (6.28) $N-n$ times, together with (6.25), gives the following formula for the n-level density:

$$\begin{aligned}
&R_n(\theta_1,\cdots,\theta_n)=\frac{N!}{(N-n)!}\int_0^\pi\cdots\int_0^\pi\frac{1}{N!}\det(f_N(\theta_j,\theta_k))_{N\times N}d\theta_{n+1}\cdots d\theta_N\\
&=\frac{1}{(N-n)!}(N-(N-1))(N-(N-2))\cdots(N-(n+1-1))\det(f_N(\theta_j,\theta_k))_{n\times n}\\
&=\det(f_N(\theta_j,\theta_k))_{n\times n}.
\end{aligned}\tag{6.29}$$

So, using (6.29) in (6.6), we arrive at

$$R_1^{T_{\mathcal{X}}}(\theta)=\frac{C_{\mathcal{X}}}{2\pi i}\int_{c-i\infty}^{c+i\infty}\frac{2^{Nr}}{C_{0,r}}\frac{\exp(-r\mathcal{X})}{r}f_N^{(r-1/2,-1/2)}(\theta,\theta)\,dr\tag{6.30}$$

with $C_{0,r}$ given in (6.24).

With the Christoffel-Darboux formula (see equation (4.5.2) in [59]) we have

$$f_N^{(r-1/2,s-1/2)}(\theta_j,\theta_k) = \frac{2^{-r-s+1}}{2(N-1)+r+s+1}\frac{\Gamma(N+1)\Gamma(N+r+s)}{\Gamma(N+r-1/2)\Gamma(N+s-1/2)}\times$$
$$\times \frac{(1+\cos\theta_j)^{s/2}(1-\cos\theta_j)^{r/2}(1+\cos\theta_k)^{s/2}(1-\cos\theta_k)^{r/2}}{\cos\theta_j-\cos\theta_k}\times$$
$$\times \Bigg[P_N^{(r-1/2,s-1/2)}(\cos\theta_j)P_{N-1}^{(r-1/2,s-1/2)}(\cos\theta_k)$$
$$- P_{N-1}^{(r-1/2,s-1/2)}(\cos\theta_j)P_N^{(r-1/2,s-1/2)}(\cos\theta_k)\Bigg]. \quad (6.31)$$

Thus $f(\theta,\theta)$ in (6.30) reduces, with the Christoffel-Darboux formula (6.31), to

$$f_N^{(r-1/2,-1/2)}(\theta,\theta) = (1-\cos\theta)^r\frac{2^{1-r}}{2N+r-1}\frac{\Gamma(N+1)\Gamma(N+r)}{\Gamma(N+r-1/2)\Gamma(N-1/2)}\times$$
$$\times \Bigg[\Big[\frac{d}{d\cos\theta}P_N^{(r-1/2,-1/2)}(\cos\theta)\Big]P_{N-1}^{(r-1/2,-1/2)}(\cos\theta)$$
$$- P_N^{(r-1/2,-1/2)}(\cos\theta)\frac{d}{d\cos\theta}P_{N-1}^{(r-1/2,-1/2)}(\cos\theta)\Bigg]$$
$$= (1-\cos\theta)^r\frac{2^{1-r}}{2N+r-1}\frac{\Gamma(N+1)\Gamma(N+r)}{\Gamma(N+r-1/2)\Gamma(N-1/2)}P(N,r,\theta), \quad (6.32)$$

where we define

$$P(N,r,\theta) := \Big[\frac{d}{d\cos\theta}P_N^{(r-1/2,-1/2)}(\cos\theta)\Big]P_{N-1}^{(r-1/2,-1/2)}(\cos\theta)$$
$$- P_N^{(r-1/2,-1/2)}(\cos\theta)\frac{d}{d\cos\theta}P_{N-1}^{(r-1/2,-1/2)}(\cos\theta). \quad (6.33)$$

With (6.32) in (6.30) we arrive at

$$R_1^{T\mathcal{X}}(\theta) = \frac{C_{\mathcal{X}}}{2\pi i}\int_{c-i\infty}^{c+i\infty}\frac{\exp(-r\mathcal{X})}{r}2^{N^2+2Nr-N}\times$$
$$\times\prod_{j=0}^{N-1}\frac{\Gamma(2+j)\Gamma(1/2+j)\Gamma(r+1/2+j)}{\Gamma(r+N+j)}\times$$
$$\times(1-\cos\theta)^r\frac{2^{1-r}}{2N+r-1}\frac{\Gamma(N+1)\Gamma(N+r)}{\Gamma(N+r-1/2)\Gamma(N-1/2)}P(N,r,\theta)\,dr. \quad (6.34)$$

□

6.4. **Proof of Theorem 1.3.**

Proof. We consider (6.34) (that is the form of $R_1^{T\mathcal{X}}$ given in Theorem 1.2). First, we observe that by [59], pages 63–64, the Jacobi polynomial $P_N^{(\alpha,\beta)}(x)$ is a polynomial in α,β and x for arbitrary complex values of α and β. Hence $P(N,r,\theta)$ is a polynomial in r.

The poles arising from $\Gamma(N+r)$ at negative integers $\leq -N$ are cancelled by the zeros of the term $1/\Gamma(r+N+j)$ for $j=0$. The pole at $r=1-2N$ of $1/(2N+r-1)$ is cancelled by the zero of $1/\Gamma(N+r+j)$ when $j=N-1$. We now discuss under which conditions we can close the contour to the left. For this, it is helpful to analyze the integrand of (6.34) when $|r|$ is large. Our main reference for various identities and formulæ in the following is [1].

Using equation (22.5.42) in [1] we write the Jacobi polynomials as

$$P_N^{(r-1/2,-1/2)}(\cos\theta) = \binom{N+r-1/2}{N} F(-N, N+r; r+1/2; \tfrac{1-\cos\theta}{2}), \tag{6.35}$$

where F is a hypergeometric function. This representation allows us to calculate the derivative of the Jacobi polynomial that appears in $P(N,r,\theta)$ using (15.2.1 in [1])

$$\frac{d}{dz}F(a,b;c;z) = \frac{ab}{c}F(a+1,b+1;c+1;z). \tag{6.36}$$

Combining the last identity with (6.35) gives

$$\begin{aligned}
&\frac{d}{d\cos\theta}P_N^{(r-1/2,-1/2)}(\cos\theta) \\
&\qquad = -\frac{1}{2}\binom{N+r-1/2}{N}\frac{d}{dz}F(-N,N+r;r+1/2;z)\Big|_{z=\frac{1-\cos\theta}{2}} \\
&= -\frac{1}{2}\binom{N+r-1/2}{N}\frac{(-N)(N+r)}{r+1/2}F(-N+1,N+r+1;r+3/2;\tfrac{1-\cos\theta}{2}).
\end{aligned} \tag{6.37}$$

Substituting (6.35) and (6.37) into (6.33) yields

$$\begin{aligned}
P(N,r,\theta) = -\frac{1}{2(r+1/2)}&\binom{N+r-1/2}{N}\binom{N+r-3/2}{N}\times \\
&\times\Big[(-N)(N+r)F(-N+1,N-1+r;r+1/2;\tfrac{1-\cos\theta}{2})\times \\
&\qquad\times F(-N+1,N+r+1;r+3/2;\tfrac{1-\cos\theta}{2}) \\
&\quad -(-N+1)(N-1+r)F(-N,N+r;r+1/2;\tfrac{1-\cos\theta}{2})\times \\
&\qquad\times F(-N+2,N+r;r+3/2;\tfrac{1-\cos\theta}{2})\Big].
\end{aligned} \tag{6.38}$$

We want the asymptotics for large $|r|$, and this is easier when r appears only in one argument of the hypergeometric function. For this, we use identity 15.3.4 from [1]:

$$F(a,b;c;z) = (1-z)^{-a}F(a,c-b;c;\tfrac{z}{z-1}), \tag{6.39}$$

and so we obtain

$$P(N,r,\theta) = -\frac{1}{2(r+1/2)}\binom{N+r-1/2}{N}\binom{N+r-3/2}{N}\Big(\frac{1+\cos\theta}{2}\Big)^{2N-2}\times \\ \times\Big[(-N)(N+r)F(-N+1,-N+3/2;r+1/2;\tfrac{\cos\theta-1}{\cos\theta+1})\times \\ \times F(-N+1,1/2-N;r+3/2;\tfrac{\cos\theta-1}{\cos\theta+1}) \\ -(-N+1)(N-1+r)F(-N,1/2-N;r+1/2;\tfrac{\cos\theta-1}{\cos\theta+1})\times \\ \times F(-N+2,3/2-N;r+3/2;\tfrac{\cos\theta-1}{\cos\theta+1})\Big]. \tag{6.40}$$

Recalling equation 15.7.1 from [1],

$$F(a,b;c;z) = \sum_{n=0}^{m}\frac{\Gamma(a+n)\Gamma(b+n)\Gamma(c)}{\Gamma(a)\Gamma(b)\Gamma(c+n)}\frac{z^n}{n!} + O(|c|^{-m-1}), \tag{6.41}$$

which holds for fixed a,b and z and large $|c|$ we get

$$F\left(-N+1,-N+3/2;r+1/2;\tfrac{\cos\theta-1}{\cos\theta+1}\right) = 1+O\big(|r|^{-1}\big), \tag{6.42}$$

and similarly for the other hypergeometric functions. Concentrating on the integrand of $R_1^{T\mathcal{X}}(\theta)$, in (6.34), and neglecting factors not depending on r, we find, using (6.42), that the growth-dependence of the integrand on r is

$$2^{2Nr}(1-\cos\theta)^r\prod_{j=0}^{N-1}\frac{\Gamma(r+1/2+j)}{\Gamma(r+N+j)}\,\frac{\exp(-r\mathcal{X})}{r}\frac{2^{-r}}{2N+r-1}\frac{\Gamma(N+r)}{\Gamma(N+r-1/2)}\times \\ \times\frac{\Gamma(N+r+1/2)\Gamma(N+r-1/2)}{\Gamma(r+1/2)\Gamma(r-1/2)}\Big[1+O\big(|r|^{-1}\big)\Big]. \tag{6.43}$$

Upon simplification, and replacing the products of Gamma functions with Barnes double Gamma functions, the growth-dependence on large $|r|$ is

$$\frac{2^{2Nr-r}}{r(2N+r-1)}\exp(r(\log(1-\cos\theta)-\mathcal{X}))\frac{G(r+1/2+N)}{G(r+3/2)}\frac{G(r+N+1)}{G(r+2N)}\times \\ \times\frac{\Gamma(N+r+1/2)}{\Gamma(r-1/2)}\Big[1+O\big(|r|^{-1}\big)\Big]. \tag{6.44}$$

Recall the asymptotic formula for $G(z)$ for large $|z|$:

$$\log G(z+1) \sim z^2(\tfrac{1}{2}\log z - \tfrac{3}{4}) + \tfrac{1}{2}z\log(2\pi) - \tfrac{1}{12}\log z + \zeta'(-1) + O(z^{-1}). \tag{6.45}$$

Applying (6.45) and Stirling's formula we conclude that the integrand in (6.34) grows like

$$\frac{1}{|r|^2}\exp(r(2N\log 2 - \log 2 + \log(1-\cos\theta) - \mathcal{X}))\Big[1+O\big(|r|^{-1}\big)\Big] \tag{6.46}$$

for large $|r|$.

From (6.46) we deduce that if $(2N-1)\log 2+\log(1-\cos\theta)-\mathcal{X} > 0$ then we can close the contour in the left half of the complex plane, thus enclosing the poles at zero and the negative half integers. If, on the other hand, $(2N-1)\log 2+\log(1-$

$\cos\theta) - \mathcal{X} < 0$ then we must close the contour in the right half-plane, implying that the integral (6.34) is zero.

Finally, we compute the residues when moving the contour to the left. There is a simple pole at $r = 0$ with residue

$$2^{N^2-N} \prod_{j=0}^{N-1} \frac{\Gamma(2+j)\Gamma(1/2+j)\Gamma(1/2+j)}{\Gamma(N+j)} \frac{2}{2N-1} \frac{\Gamma(N+1)\Gamma(N)}{\Gamma(N-1/2)\Gamma(N-1/2)} \times \\ \times P(N, 0, \theta). \quad (6.47)$$

Note that when $r = 0$ the expression for $P(N, r, \theta)$ reduces to that corresponding to $\mathrm{SO}(2N)$.

There is also a simple pole at $r = -1/2$ with residue

$$-2\exp(\mathcal{X}/2)2^{N^2-2N+3/2} \frac{(1-\cos\theta)^{-1/2}}{2N-3/2} \frac{\Gamma(N+1)\Gamma(1/2)}{\Gamma(N-1)\Gamma(N-1/2)} \times \\ \times \prod_{j=1}^{N-1} \frac{\Gamma(2+j)\Gamma(1/2+j)\Gamma(j)}{\Gamma(N+j-1/2)} P(N, -1/2, \theta). \quad (6.48)$$

Similarly to (6.17), where we determined the normalization constant $C_{\mathcal{X}}$, the contribution from the residues of the higher order poles at $\alpha_k = \frac{-1-2k}{2}$ with $k = 1, 2, 3, \ldots$ is

$$\sum_{k\geq 1}^{\infty} b_k \exp((k+1/2)\mathcal{X}) \quad (6.49)$$

where the coefficients b_k come from the residues. □

To show convergence we may write the series (6.49) as

$$\sum_{1\leq k\leq K} b_k \exp((k+1/2)\mathcal{X}) + \int_{c_K - i\infty}^{c_K + i\infty} \exp(-r\mathcal{X}) f(r) dr \quad (6.50)$$

where $\exp(-r\mathcal{X})f(r)$ is the integrand in (6.34) and $\alpha_{K+1} < c_K < \alpha_K$. By (6.46), $f(r) \ll \exp(-rX)$ for large $|r|$ and $\mathcal{X} < 0$. Thus,

$$\int_{c_K - i\infty}^{c_K + i\infty} \exp(-r\mathcal{X}) f(r) dr = \exp(-c_K\mathcal{X}) i \int_{-\infty}^{\infty} \exp(-it\mathcal{X}) f(c_K + it) dt \\ = O(\exp(-c_K\mathcal{X})). \quad (6.51)$$

Hence, the contributions of residues of higher poles decrease exponentially fast for $\mathcal{X} < 0$ and using only the K right-most poles gives an error that is $O(\exp(-c_K\mathcal{X}))$. The computation of residues of higher order poles can be carried out by computer algebra. We find that for reasonable $\mathcal{X}$ we have good convergence using about 10 poles.

Remark 6.1. The hard gap reflected in Theorem 1.3 may be understood as follows. Recalling that $\Lambda_A(1, N) = 2^N \prod_{n=1}^{N}(1-\cos\theta_n)$ it follows that $\log\Lambda_A(1, N) = (2N-1)\log 2 + \log(1-\cos\theta)$ for the matrix $A \in \mathrm{SO}(2N)$ having $2N-2$ eigenvalues at -1 (i. e., $\theta_2, \ldots, \theta_N = \pi$) and a symmetric pair of eigenvalues at $e^{\pm i\theta}$ (i. e., $\theta_1 = \theta$). Plainly, such matrix A maximizes $\log\Lambda_A(1, N)$ subject to the condition

that a pair of eigenvalues lie at $e^{\pm i\theta}$. Therefore, for any fixed $\mathcal{X}$, the condition $\log \Lambda_A(1,N) > \mathcal{X}$ implies $\mathcal{X} < (2N-1)\log 2 + \log(1-\cos\theta)$: if the latter inequality does not hold, there are *no* matrices A with $\log \Lambda_A(1,N) > \mathcal{X}$. In particular, for fixed N and $\mathcal{X}$ there is a lower bound for all eigenphases θ of any matrix A with $\log \Lambda_A(1,N) > \mathcal{X}$, namely $\theta > \theta_{\text{inf}} := \cos^{-1}(1 - 2^{-(2N-1)}e^{\mathcal{X}})$: the excised one-level density is identically zero in the excluded spectral interval ("hard gap") $\theta \le \theta_{\text{inf}}$. Note that the hard gap shrinks to zero exponentially fast as $N \to \infty$ and also as $\mathcal{X} \to -\infty$.

6.5. **Formula vs. data.** For illustration and as a consistency test, in figure 13 we compare our formula for the one-level density with data obtained by generating random matrices from the excised ensemble SO($2N$).

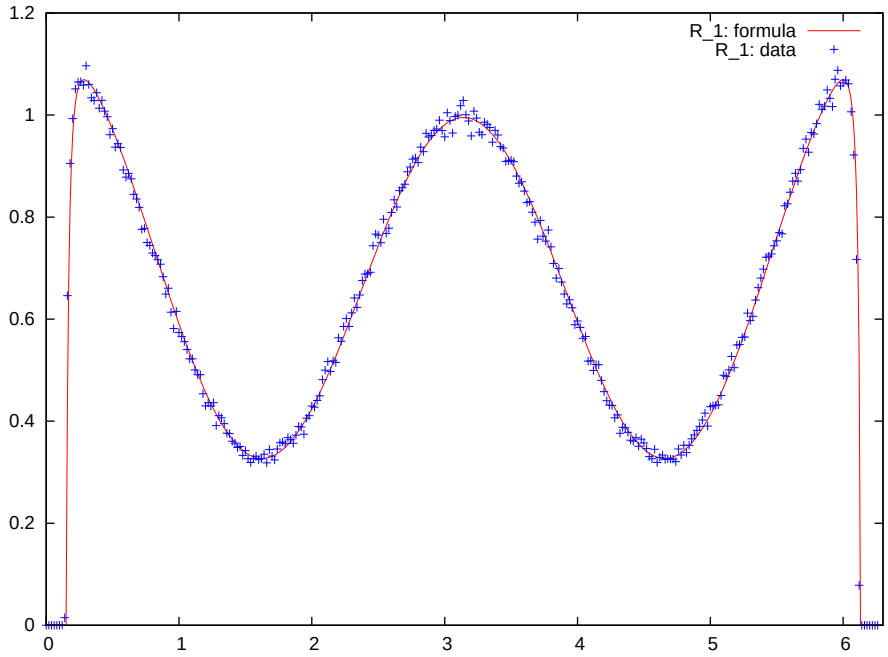

FIGURE 13. One-level density of excised SO($2N$), $N = 2$ with cutoff $|\Lambda_A(1,N)| \ge 0.1$. The *red curve* uses our formulæ from Theorems 1.2 and 1.3. The *blue crosses* give the empirical one-level density of 200,000 numerically generated matrices.

7. REFERENCES

[1] M. Abramowitz and I.A. Stegun. *Handbook of Mathematical Functions*. Dover Publications, Inc., New York, 1965.
[2] E.W. Barnes. The theory of the G-function. *Q. J. Math.*, 31:264–314, 1900.
[3] E. M. Baruch and Z. Mao. Central value of automorphic L-functions. *Geom. Func. Anal.*, 17:333–384, 2007.
[4] M.V. Berry and J.P. Keating. The Riemann zeros and eigenvalue asymptotics. *SIAM Rev.*, 41:236–266, 1999.

[5] E. Bogomolny, O. Bohigas, P. Leboeuf, and A.G. Monastra. On the spacing distribution of the Riemann zeros: corrections to the asymptotic result. *J. Phys. A*, 39:10743–10754, 2006. (E-print: `math.NT/0602270`).

[6] E.B. Bogomolny and J.P. Keating. Gutzwiller's trace formula and spectral statistics: beyond the diagonal approximation. *Phys. Rev. Lett.*, 77:1472–1475, 1996.

[7] H.M. Bui and J.P. Keating. On the mean values of Dirichlet L-functions. *Proc. London. Math. Soc.*, 95:273–298, 2007.

[8] H.M. Bui and J.P. Keating. On the mean values of l-functions in orthogonal and symplectic families. *Proc. London. Math. Soc.*, 96:335–366, 2008.

[9] J.B. Conrey. *Recent Perspectives on Random Matrix Theory and Number Theory*, volume 322 of *London Math. Soc. Lecture Note Ser.*, chapter Note on eigenvalue distributions for the classical compact groups, pages 111–145. Cambridge University Press, 2005.

[10] J.B. Conrey and D.W. Farmer. Mean values of L–functions and symmetry. *Internat. Math. Res. Notices*, 17:883–908, 2000.

[11] J.B. Conrey, D.W. Farmer, J.P. Keating, M. O. Rubinstein, and N.C. Snaith. Integral moments of L-functions. *Proc. Lond. Math. Soc.*, 91:33–104, 2005.

[12] J.B. Conrey, D.W. Farmer, and M.R. Zirnbauer. Autocorrelation of ratios of L-functions. *Comm. Number Theory and Physics*, 2(3):593–636, 2008. `arXiv:0711.0718`.

[13] J.B. Conrey, J.P. Keating, M.O. Rubinstein, and N.C. Snaith. On the frequency of vanishing of quadratic twists of modular L-functions. In *Number theory for the millennium, I (Urbana, IL, 2000)*, pages 301–315. A K Peters, Natick, MA, 2002.

[14] J.B. Conrey, J.P. Keating, M.O. Rubinstein, and N.C. Snaith. Random matrix theory and the Fourier coefficients of half-integral weight forms. *Experimental Math.*, 15:67–82, 2006. Preprint: `math.NT/0412083`.

[15] J.B. Conrey, M.O. Rubinstein, and N.C. Snaith. Moments of the derivative of characteristic polynomials with an application to the Riemann zeta-function. *Comm. Math. Phys.*, 267(3):611–629, 2006. `arXiv:math.NT/0508378`.

[16] J.B. Conrey, M.O. Rubinstein, N.C. Snaith, and M. Watkins. Discretisation for odd quadratic twists. In *Ranks of Elliptic Curves and Random Matrix Theory, LMS lecture note series 341*, pages 201–214. Cambridge University Press, Cambridge, 2007. `arXiv:math.NT/0509428`.

[17] J.B. Conrey and N.C. Snaith. Applications of the L-functions ratios conjectures. *Proc. Lon. Math. Soc.*, 94 (3):594–646, 2007. (E-print: `math.NT/0509480`).

[18] J.B. Conrey and N.C. Snaith. Correlations of eigenvalues and Riemann zeros. *Comm. Number Theory and Phyics*, 2(3):477–536, 2008. `arXiv:0803.2795`.

[19] J.B. Conrey and N.C. Snaith. Triple correlation of the Riemann zeros. *J. Theor. Nombres Bordeaux*, 20:61–106, 2008.

[20] E. Dueñez, D.K. Huynh, J.P. Keating, S.J. Miller, and N.C. Snaith. The lowest eigenvalue of Jacobi random matrix ensembles and Painlevé VI. *J. Phys. A: Math. Theor.*, 43:405204, 2010.

[21] E. Dueñez and S.J. Miller. The low lying zeros of a $GL(4)$ and a $GL(6)$ family of L-functions. *Compositio Mathematica*, 142(06):1403–1425, 2006.
[22] D.W. Farmer, S. M. Gonek, and C.P. Hughes. The maximum size of L-functions. *Journal für die reine und angewandte Mathematik*, 609:215–36, 2007.
[23] P. J. Forrester and N. S. Witte. Application of the τ-function theory of Painlevé equations to random matrices: P_{VI}, the JUE, CyUE, cJUE and scaled limits. *Nagoya Math. J.*, 174:29–114, 2004.
[24] Peter J. Forrester. *Log-Gases and Random Matrices*. Princeton University Press, 2010.
[25] E. Fouvry and H. Iwaniec. Low-lying zeros of dihedral L-functions. *Duke Math. J.*, 116:189–217, 2003.
[26] J. Goes and S. J. Miller. Towards an 'average' version of the Birch and Swinnerton-Dyer Conjecture. *Journal of Number Theory*, 130:2341–2358, 2010.
[27] S.M. Gonek, C.P. Hughes, and J.P. Keating. A hybrid Euler-Hadamard product formula for the Riemann zeta function. *Duke Math. J.*, 136(3):507–550, 2007.
[28] A. M. Güloğlu. Low-lying zeros of symmetric power L-functions. *Internat. Math. Res. Not.*, 2005:517–550, 2005.
[29] C.P. Hughes. Random matrix theory and discrete moments of the Riemann zeta function. *J. Phys. A.*, 36:2907–2917, 2003.
[30] C.P. Hughes. Mock-Gaussian behaviour. In F. Mezzadri and N.C. Snaith, editors, *Recent Perspectives in Random Matrix Theory and Number Theory*, volume 322 of *London Mathematical Society Lecture Note Series*, pages 337–355, 2005.
[31] C.P. Hughes, J.P. Keating, and N. O'Connell. Random matrix theory and the derivative of the Riemann zeta function. *Proc. R. Soc. Lond. A*, 456:2611–2627, 2000.
[32] C.P. Hughes and S.J. Miller. Low-lying zeros of L-functions with orthogonal symmetry. *Duke Math. J.*, 136:115–172, 2007. (E-print: `math.NT/0507450`).
[33] C.P. Hughes and Z. Rudnick. Linear statistics for zeros of Riemann's zeta function. *C. R. Acad. Sci. Paris, Ser. I*, 335:667–670, 2002.
[34] C.P. Hughes and Z. Rudnick. Linear statistics of low-lying zeros of L-functions. *Quart. J. Math*, 54:309–333, 2003.
[35] C.P. Hughes and Z. Rudnick. Mock-Gaussian behaviour for linear statistics of classical compact groups. *J. Phys. A.*, 36:2919–2932, 2003.
[36] D. K. Huynh. *Elliptic curve L-functions of finite conductor and random matrix theory*. PhD thesis, University of Bristol, 2009.
[37] D.K. Huynh, J.P. Keating, and N.C. Snaith. Lower order terms for the one-level density of elliptic curve L-functions. *Journal of Number Theory*, 129(12):2883–2902, 2009.
[38] D.K. Huynh, S.J. Miller, and R. Morrison. An elliptic curve family test of the ratios conjecture. *Journal of Number Theory*, 131:1117–1147, 2011.

[39] H. Iwaniec, W. Luo, and P. Sarnak. Low lying zeros of families of L-functions. *Inst. Hautes Études Sci. Publ. Math.*, 91:55–131, 2000.
[40] N.M. Katz and P. Sarnak. *Random Matrices, Frobenius Eigenvalues, and Monodromy*. AMS Colloquium Publications, 1999.
[41] N.M. Katz and P. Sarnak. Zeros of zeta functions and symmetry. *Bull. Amer. Math. Soc.*, 36:1–26, 1999.
[42] J.P. Keating and N.C. Snaith. Random matrix theory and $\zeta(1/2+it)$. *Comm. Math. Phys.*, 214:57–89, 2000.
[43] J.P. Keating and N.C. Snaith. Random matrix theory and L–functions at $s = 1/2$. *Comm. Math. Phys.*, 214:91–110, 2000.
[44] W. Kohnen and D. Zagier. Values of L-series of Modular Forms at the Center of the Critical Strip. *Invent. math.*, 64:175–198, 1981.
[45] S. Marshall. Zero repulsion in families of elliptic curve L-functions and an observation of S. J. Miller. *Preprint*. `arXiv:1109.0224`.
[46] M.L. Mehta. *Random Matrices*. Academic Press, 2nd edition, 1991.
[47] F. Mezzadri. Random matrix theory and the zeros of $\zeta'(s)$. *J. Phys. A: Math. Gen.*, 36:2945–2962, 2003.
[48] S.J. Miller. *1- and 2-level densities for families of elliptic curves: Evidence for the underlying group symmetries*. PhD thesis, Princeton University, 2002.
[49] S.J. Miller. One- and two-level densities for rational families of elliptic curves: evidence for the underlying group symmetries. *Compos. Math.*, 140:952–992, 2004.
[50] S.J. Miller. Investigations of zeros near the central point of elliptic curve L-functions. *Experiment. Math.*, 15 (3):257–279, 2006. (E-print: `math.NT/0508150`).
[51] S.J. Miller. Lower order terms in the 1-level density for families of holomorphic cuspidal newforms. *Acta Arith.*, 137(1):51–98, 2009.
[52] S.J. Miller and R. Peckner. Low-lying zeros of number field L-functions. (E-print: http://arxiv.org/abs/1003.5336), 2010.
[53] A. E. Özlük and C. Snyder. On the distribution of the nontrivial zeros of quadratic L-functions close to the real axis. *Acta Arith.*, 91(3):209–228, 1999.
[54] G. Ricotta and E. Royer. Lower order terms for the one-level densities of symmetric power L-functions in the level aspect. *Acta Arith.*, 141(2):153–170, 2010. `arXiv:0806.2908`.
[55] E. Royer. Petits zéros de fonctions L de formes modulaires. *Acta Arith*, 99(2):147–172, 2001.
[56] M.O. Rubinstein. The L-function software and zeros/values database, `http://pmmac03.math.uwaterloo.ca/mrubinst/L_function_public/L.html`.
[57] M.O. Rubinstein. Low-lying zeros of L-functions and random matrix theory. *Duke Math. J.*, 109:147–181, 2001.
[58] N.C. Snaith. Derivatives of random matrix characteristic polynomials with applications to elliptic curves. *J. Phys. A: Math. Gen.*, 38:10345–10360, 2005. (E-print: `math.NT/0508256`).
[59] G. Szegő. *Orthogonal Polynomials*. AMS Colloquium Publications XXII, 1939.

[60] J.L. Waldspurger. Correspondances de Shimura et Shintani. *J. Math. pures et appl.*, 59:1–133, 1980.
[61] H. Weyl. *Classical Groups*. Princeton University Press, 1946.
[62] M. P. Young. Low-lying zeros of families of elliptic curves. *J. Amer. Math. Soc.*, 19:205–250, 2006.

E-mail address: eduenez@math.utsa.edu

Department of Mathematics, University of Texas at San Antonio, San Antonio, TX 78249, USA

E-mail address: dkhuynhms@gmail.com

Department of Pure Mathematics, University of Waterloo, Waterloo, ON, N2L 3G1, Canada

E-mail address: J.P.Keating@bristol.ac.uk

School of Mathematics, University of Bristol, Bristol BS8 1TW, UK

E-mail address: Steven.J.Miller@williams.edu

Department of Mathematics and Statistics, Williams College, Williamstown, MA 01267, USA

E-mail address: N.C.Snaith@bristol.ac.uk

School of Mathematics, University of Bristol, Bristol BS8 1TW, UK